CENTRAL INSTITUTE FOR INDUSTRIAL RESEARCH

Oslo - Blindern, Norway

Central Institute for Industrial Research
Blindern, Oslo, Norway

ANNUAL TECHNICAL REPORT

Contract No. DA-91-591-EUC-2077

KINETICS OF METAL/METAL-ION ELECTRODES IN AQUEOUS SOLUTIONS

Tor Hurlen

Period covered:

January 1 - December 31, 1962

62 01 01

The research reported in this document has been made possible through the support and sponsorship of the U.S. Department of Army, through its European Research Office.

The present Annual Technical Report of Contract No. Da-91-591-EUC-2077 is a collection of the three Special Scientific Reports made during the contract period. These three reports cover the main part of the work done under the contract and are entitled:

1. Kinetics of Metal/Metal-Ion Electrodes: Iron, Copper, Zinc.
2. Anodic Behaviour of Iron in Alkaline Solutions.
3. Radiochemical Studies on the Cu/Cu^{2+}_{aq} Electrode.

The first of these is also published in Electrochimica Acta 7 (1962) 653.

Some work has moreover been done on the reactions of the Mn/Mn^{2+}_{aq} electrode, but we have not succeeded in carrying this work far enough to describe it in the present report. A special report on manganese will therefore be prepared as soon as possible.

Blinder, Norway
January 1963

Tor Hurlen

Tor Hurlen
Principal Investigator

SI Publ. No. 392
Proj. No. 62 01 01

Special Scientific Report No. 3
Contract No. DA-91-591-EUC-2077

RADIOCHEMICAL STUDIES ON THE Cu/Cu^{2+}_{aq} ELECTRODE

T. Hurlen and G. Lunde

January 1963

The research reported in this document has been made possible through the support and sponsorship of the U.S. Department of Army, through its European Research Office.

Central Institute for Industrial Research
Blindern, Oslo, Norway

St. 3671

RADIOTRACER STUDIES ON THE Cu/Cu^{2+}_{aq} ELECTRODE

T. Hurlen and G. Lunde

CENTRAL INSTITUTE FOR INDUSTRIAL RESEARCH

BLINDERN, OSLO, NORWAY

ABSTRACT

Experiments are made on the effect of dissolution on the pickup of radioactivity by copper sheets in sulphuric acid solutions of radioactive (^{64}Cu) cupric sulphate at 20 °C. The results are discussed both on the basis of an intermediate cuprous ion model and on the basis of a crystal growth involving direct cupric ion model for the copper/cupric reactions. They are found to be well in accordance with the latter. Data are further obtained for the exchange current and for the absolute rate of dissolution and deposition at various anodic overvoltages and net dissolution rates. The exchange is found to concern about one atomic layer on the metal surface.

St. 3671

1.0 INTRODUCTION

Radiochemical methods have already been widely used in the study of exchange reactions between metals and their ions in aqueous solutions (see e.g. Refs. 1-4 where further references are given).

Many early measurements of this kind[1] clearly are affected by corrosion and by the formation of solid corrosion products on the metal surface. Som of these concern copper in not acidified cupric sulphate and chloride solutions, and it is now well known that there on a copper surface in such solutions is a formation of cuprous oxide[5] and chloride[6], respectively. In the latter case, there further is a strong dissolution of copper[7]. This largely invalidates many of the early conclusions, some of which also are in disagreement with electrochemical data. In the present work, therefore, studies are made on the exchange of copper with cupric ions in acidified sulphate solutions which are low enough in pH to avoid cuprous oxide formation.

One of the main objects of radiochemical exchange studies is to have a direct determination of the rate of exchange. In most previous work, such determinations have been attempted through measurements on the time dependence of the pickup of radioactivity by the initially inactive phase (which for meaningful measurements ought to be the metal phase[2-4]). As shown by Gerischer et al.[2,3] and King et al.[4], however, this time dependence may often be affected by other factors than the pure exchange (e.g. diffusion of tracers) and can mainly give a lower limit for the exchange rate. Gerischer and Tischer[3] have further shown how a higher limit often can be determined from the essentially stationary amount of radioactivity acquired by a metal when dissolving in a radioactive solution of its ions. In the present work, the latter approach has been applied, and it is shown how this also can be used for an evaluation of the kinetics of the exchange reactions.

In the work by Gerischer and Tischer, the dissolution was generated and controlled by applied anodic currents. This has the disadvantage that the anodic dissolution necessarily has to cease before the metal can be freed from the radioactive solution by washing. In the present

work, this is improved by the dissolution being generated and controlled by an oxidation agent in the solution. Ferric sulphate is used for this purpose, as this agent previously has been shown to have no influence on the dissolution mechanism[8].

2.0 THEORETICAL

It is well known that copper in acidified cupric sulphate solutions essentially acts as a Cu/Cu^{2+}_{aq} electrode. Different opinions are held, however, whether its reactions occur mainly through an intermediate formation of cuprous ions[9,10]:

$$Cu = Cu^{+} + e^{-} \qquad (1)$$

$$Cu^{+} = Cu^{2+} + e^{-} \qquad (2)$$

with (2) as the rate-determining reaction, or mainly by a direct transfer of cupric ions[11,12]:

$$Cu = Cu^{2+} + 2e^{-} \qquad (3)$$

with (2) as an essentially non-interfering side reaction. In the following, it shall be shown how a distinction can be made between these two possibilities by radiochemical studies.

From previous results[3,4] (and also from those to be described below), it is known that the exchange between a metal and its ions in aqueous solutions in one way or another concerns all surface atoms (and not only a part corresponding to the variable number of step or kink atoms in the surface), and that the diffusion of atoms from the surface into the metal is slow enough to be neglected in the below treatment. On this basis, it is easily seen that the stationary number (n^{*}) of tracer atoms acquired by a copper crystal when dissolving in a tracer solution of cupric sulphate, with good approximation should be given by[3]:

$$n^{*}/n^{*}_{o} = (i_{-}/i_{+})\left(1 + \frac{i}{i_{lim}}\right)^{-1} \qquad (4)$$

where i is the net dissolution rate; i_{lim} is the limiting current for copper deposition; i_{+} and i_{-} are the absolute rate in anodic and cathodic direction, respectively, of the rate-determining reaction of the copper/cupric electrode; and n^{*}_{o} is the stationary number of tracer atoms acquired by the crystal when in electrochemical equilibrium

with the cupric ions of the solution (i=0). The first factor on the right hand side of (4) represents the relative cupric tracer concentration at the copper surface under stationary conditions as compared to its value in the bulk of the solution. In deriving (4), we have further regarded the dissolution rate as equal to the net anodic rate of the rate-determining reaction for the copper/cupric electrode:

$$i = i_+ - i_- \qquad (5)$$

This is known to be a sufficiently valid approximation, both in case of intermediate cuprous ion formation[9,10] and in case of direct cupric ion transfer[11]. By (4) and (5), it should thus be possible to determine both i_+ and i_- at various dissolution rates and limiting current conditions.

Overvoltage and Pickup.

Both the purely electrochemical intermediate cuprous ion model of Bockris et al.[9,10] and the crystal growth involving direct cupric ion model of Hurlen[11,12] imply:

$$i_-/i_+ = (1+ \frac{i}{i_{lim}}) \exp(\frac{2F}{RT}(E-V)) \qquad (6)$$

which by combination with (4) gives:

$$n^*/n_o^* = \exp(\frac{2F}{RT}(E-V)) \qquad (7)$$

where V is the actual potential and E the reversible potential of copper in the solution applied. From combined potential and radiochemical data of the present kind, no distinction can therefore be made between the two models. Such data are nevertheless of interest in testing the validity of (7).

Dissolution and Pickup.

The intermediate cuprous ion model and the direct cupric ion model respectively imply:

$$i/i_o = \exp(\frac{3F}{2RT}(V-E)) - (1+ \frac{i}{i_{lim}}) \exp(\frac{F}{2RT}(E-V)) \qquad (8a)$$

$$2i/i_o = \exp(\frac{2F}{RT}(V-E)) - (1+ \frac{i}{i_{lim}})^2 \exp(\frac{2F}{RT}(E-V)) \qquad (8b)$$

where i_o is the reversible exchange current for the rate-determining reaction of the copper/cupric electrode. By combining these equations with (7), we have:

$$i/i_o = (n_o^*/n^*)^{3/4} - (1+ \frac{i}{i_{lim}})(n^*/n_o^*)^{1/4} \qquad (9a)$$

$$2i/i_o = (n_o^*/n^*) - (1+ \frac{i}{i_{lim}})^2 (n^*/n_o^*) \qquad (9b)$$

for the two respective models. These equations show that the radioactive pickup should be little affected by the dissolution rate when low compared to i_o and i_{lim}, and that it with increasing dissolution rate should approach:

$$n^*/n_o^* = (i_o/i)^{4/3} \qquad (10a)$$

$$2n^*/n_o^* = i_o/i \qquad (10b)$$

for the two respective models in case $i_o << i_{lim}$, and

$$n^*/n_o^* = i_{lim}/i \qquad (11)$$

for both models in case $i_o >> i_{lim}$.

From electrochemical data[9-11], it is known that the former case is the most actual one (at least at not too low cupric ion concentrations). A distinction between the two models and a determination of i_o should thus be possible on the basis of equations (10).

3.0 EXPERIMENTAL

The experiments have all been performed at room temperature (about 20 °C) and with initially radio-inactive copper sheets in the following type of solutions:

$$H_2SO_4(0.1N) + CuSO_4(0.001\text{-}0.1M) + Fe_2(SO_4)_3(0\text{-}0.1M)$$

For the radiochemical measurements, part of the cupric sulphate was neutron activated for 24 h at a flux of about 10^{12} neutrons/cm^2 sec. The main radioactive copper isotop thereby formed is ^{64}Cu with $t_{1/2}$ = 12.8 h. The disintegration rates measured in the present work, both for the radioactive solutions and for the radioactive pickup by copper sheets in these solutions, were well in accordance with this half-life.

The isotope ^{66}Cu with $t_{1/2}$ = 5.8 min is also formed by the neutron activation, but this is of no importance for the present measurements.

The materials used were high purity copper sheets (Fe 2 ppm, Ag 2 ppm, Pb 1 ppm, Ni 1 ppm, Si 1 ppm, Na 1 ppm, and less than 1 ppm each of Ca and Mg, other metallic elements and O, S, Se, Te, and P being absent or below the limits of detection by the spectrographic, chemical, and metallographic methods applied) and solutions prepared from A.R. quality acid and salts in water distilled from a rather pure tap water. The copper sheets were ca 0.2 mm thick and 1x2 cm in size (surface area 4 cm^2) and had a small hole for suspension. After fabrication, they were vacuum annealed for one hour at 700 °C, mechanically polished, etched in dilute nitric acid, washed in running water and distilled water, dried with acetone, and stored in a desiccator until used.

The methods used for potential and dissolution rate measurements essentially are those previously described[7,8]. For the dissolution rate, these were supplemented and checked by determinations of the weight loss of copper sheets in the actual radiochemical experiments.

The latter experiments were performed in 100 ml pyrex beakers filled with the test solution, into which sheets were fully immersed and suspended by means of thin quartz hooks. In the main experiments, the immersion time was 10 min, and each 100 ml portion of solution was then used for maximum three single immersions (many of them for one and two only). No stirring was applied in the solution.

In some preliminary experiments, the copper sheets were kept in a radio-inactive solution of the same composition as the test solution for periods up to 24 h prior to the actual experiments. This pre-immersion, however, was not found to be of any importance for the stationary amount of radioactivity acquired by the sheets. In most of the main experiments, therefore, such a pre-immersion was not performed. The preliminary experiments further showed an immersion time of 10 min to be more than enough for essentially steady radiochemical conditions to be attained in all cases concerned in the present work.

After immersion in the test solution, the copper sheet was rapidly transferred to a 1 l beaker with tap water where it was immersed under gentle stirring for 20 sec. This washing was followed by equal washings in 1 l distilled water and 200 ml acetone, whereafter the sheet was allowed to dry in the air before being counted. Repetitions of this washing procedure with the same sheet and with intermediate countings showed it to give only a slight reduction of the pickup. The countings after one washing cycle was therefore regarded representative for the pickup. During the experiments, the wash water and acetone were frequently renewed.

The radiochemical experiments have been performed with ten different copper sheets, all of which have been used with each test solution. As moreover each test solution was prepared twice, each test condition has thereby been covered by twenty individual measurements of the radioactive pickup. The results given below are the average of these measurements.

When going from one test solution to another, the then already radioactive copper sheets were sometimes first de-activated by immer-

sion in a radio-inactive solution of the same composition as the test solution to be used. This de-activation, however, was found unnecessary by being of no importance for the stationary amount of radioactivity shown by the sheets after immersion in the new test solution.

The radioactive countings were performed by means of a Tracerlab scintillation detector with a well-type tallium activated sodium iodide crystal (2x1.75 inches). The copper sheets were counted in a standard counting tube. The background counting on the empty tube was about 300 counts/min all through the measurements. Most sample countings were from 10 to 100 times higher than this.

Estimations of the amount of copper exchanged were made on the basis of countings on a known amount of the test solution applied after diluting this with distilled water. These countings were made on 2 ml portions of the diluted solution in the same type of counting tubes as above. The difference in counting geometry for copper sheets and these solutions introduces a small failure in the direct comparison. This failure was in the present case found to be small enough to be neglected.

4.0 RESULTS

Eight of the ten copper sheets used in the present work generally gave results with an average deviation of about $\pm$ 5 % for the stationary radioactive pickup from the various solutions. For one reason or another, the remaining two sheets always deviated distinctly more (generally about 25 %) from the average, the one always in positive and the other always in negative direction. For the relative pickup (n^*/n^*_o) in a corrosive (ferric containing) solution as compared to that in the corresponding non-corrosive (ferric free) solution, however, all ten sheets generally gave results within $\pm$ 5 % of the average.

Pickup at Equilibrium

Experiments have been made in 0.1 N sulphuric acid solutions of cupric sulphate at concentrations of 0.001, 0.01, and 0.1 M. In these ferric free sclutions, copper essentially attains electrochemical equilibrium with the cupric ions by its net dissolution rate (ca. 10^{-5} A/cm^2) being lower than the copper/cupric exchange rate (around 10^{-4} A/cm^2 according to Ref.[11]). The net dissolution is here presumably caused mainly by reduction of dissolved oxygen and to some extent by reduction of cupric to coprous ions.

An essentially stationary amount of radioactivity was here acquired by the copper sheets in a rather short time. This occured in less than two minutes at the lowest cupric concentration and in less than a few seconds (the shortest immersion time applied) at the highest cupric concentration. In the latter solution, immersions of duration to fifteen hours did not show any noticable increase in the pickup.

The stationary amount of radioactive pickup was here further found to be independent of the cupric concentration and to correspond to complete exchange of one or two atomic layers on the copper surface with the solution. The latter is based on the tracer ratio having been assumed the same in the exchanged layers as inthe test solution, and on no regard having been made of the true surface area of the sheets possibly being different from the apparent one. It does not seem unreasonable that the values higher than one for the number of exchanged layers

mainly are due to differences of the latter kind, and that the exchange actually concerns one atomic layer only. This further implies that the diffusion of tracer atoms into deeper lying copper layers is negligibly slow under the conditions concerned.

Pickup during Dissolution

Experiments have been made with additions of ferric sulphate to the above solutions. This causes copper to dissolve in the solutions and to exhibit an anodic overvoltage when the dissolution is fast enough.

In Figs. 1 and 2, the results obtained for the stationary pickup in the ferric containing solutions are presented as a function of the overvoltage (Fig. 1) and of the dissolution rate (Fig. 2). The pickup is there given in relation to what it is in the ferric free solutions, and this is assumed to represent the ratio n^*/n_o^* introduced in the theoretical section above.

The line drawn in Fig. 1 is the one prescribed by the theoretical relationship (7) between overvoltage and pickup, and the relatively good fit of the experimental points to this line lends confidence to its correctness. The lines in Fig. 2 are drawn with the slope prescribed by the theoretical relationships (10b) and (11) between dissolution rate and pickup, and these may seem to fit the experimental results reasonably well at sufficiently high dissolution rates. The slope of the relationship (10a) is easily seen to give a distinctly poorer fit. At sufficiently high dissolution rates, the present results thus give:

$$n^*/n_o^* = i_x/i \qquad (12)$$

where i_x is the current obtained by extrapolating the lines in Fig. 2 to $n^*/n_o^* = 1$. It is further seen that the pickup is little affected by the dissolution when this is slow compared to i_x.

The above results apply to unstirred solutions. Stirring should here be expected to raise the net dissolution rate and the limiting current for copper deposition by mutually the same factor, but to have no

effect on the copper/cupric exchange current. Through the effect of stirring on the pickup, it should thus be possible to decide whether i_x(12) is controlled by the exchange (10b) or by diffusion (11) of cupric ions. Proper stirring experiments of this kind are rather difficult to perform, however, as the pickup varies rapidly with the conditions which may change towards those of no stirring when the sheets are transferred from the test solution to the wash water. A few such experiments have nevertheless been carried out. A magnetic stirrer was used, and the sheets were transferred to the wash beaker through a heavy stream of water which, at the moment of transfer, was poured directly into the stirred test solution. The results obtained were not well reproducible, but were though clear enough in indicating that i_x represents $i_o/2$ rather than i_{lim}.

In Fig. 3, the values obtained for i_o on this basis are plotted versus the reversible potential of copper (as measured in the ferric free solutions). When the Nernst equation is considered and the value of 0.337 V (NHS) is accepted for the standard copper/cupric potential, these results give:

$$i_o = 0.1 \cdot \underline{a} \ \ A/cm^2 \qquad (13)$$

showing the exchange current to vary linearly with the cupric activity $\underline{a}$. This is qualitatively in accordance with what to be expected from the direct cupric ion model underlying (10b) and thus supports the interpretation given for i_x. Quantitatively, (13) gives somewhat higher values for the exchange current than previously found by purely electrochemical measurements[11,12] (about $0.05 \cdot \underline{a}$ A/cm^2, when values obtained by direct extrapolation of Tafel lines are doubled[12]).

5.0 DISCUSSION

The above results are clearly in favour of the crystal growth involving direct cupric ion model described by Hurlen[12]. This model may also be called a chain reaction model as it represents a mechanism in which preferred reaction sites are formed by a direct electrochemical reaction at less preferred sites (initiation reaction) and act as chain carriers for a further direct reaction at the preferred sites (propagation reaction) until they disappear (termination reaction). In accordance with crystal growth theories, the preferred sites are assumed to be kinks (ends of atom rows) in crystal steps in the surface. Both for copper and for a number of other metals, experimental results indicate that the steady-state concentration of preferred sites varies with the electrode potential as does the sum of the absolute rates of a first-order dissolution and deposition[12]. This gives for the present case (assuming $\alpha = \frac{1}{2}$):

$$s = \frac{1}{2}\, s_R \left[\exp\left(\frac{F}{RT}(V-E)\right) + \left(1+\frac{i}{i_{lim}}\right) \exp\left(\frac{F}{RT}(E-V)\right)\right] \quad (14)$$

where s_R is the concentration of preferred sites at equilibrium (i.e. at $i = 0$ and $V = E$). A purely theoretical evaluation of this steady-state concentration has so far not been performed as this would require a clearer picture especially of the termination reaction than is presently available.

Accepting for the present the relationship (14) and assuming the propagation reaction to be the by far most frequently occuring one, we have for the absolute rate of dissolution and deposition and for the net dissolution rate under steady-state conditions[12] (assuming $\alpha = \frac{1}{2}$):

$$i_+ = \frac{1}{2}\, i_o \left[\exp\left(\frac{2F}{RT}(V-E)\right) + \left(1+\frac{i}{i_{lim}}\right)\right] \quad (15a)$$

$$i_- = \frac{1}{2}\, i_o \left[\left(1+\frac{i}{i_{lim}}\right)^2 \exp\left(\frac{2F}{RT}(E-V)\right) + \left(1+\frac{i}{i_{lim}}\right)\right] \quad (15b)$$

$$i = \frac{1}{2}\, i_o \left[\exp\left(\frac{2F}{RT}(V-E)\right) - \left(1+\frac{i}{i_{lim}}\right)^2 \exp\left(\frac{2F}{RT}(E-V)\right)\right] \quad (15c)$$

In Figs. 4 and 5, polarization curves calculated from these equations are compared with polarization points obtained from the present experimental results on the basis of (4) and (5). The relatively good fit there shown lends further confidence to the applicability of the reaction model here discussed.

In obtaining the results in Figs. 4 and 5, we have for the three different cupric concentrations used the i_o-values 0.12, 0.6, and 3.6 mA/cm^2, respectively, and the i_{lim}-values 0.18, 1.8, and 18 mA/cm^2, respectively. The i_o-values are those experimentally obtained in the present work (Fig. 3), whereas the i_{lim}-values have been chosen so as to give the best fit and to be mutually in accordance with the known concentration dependence for limiting diffusion currents. The i_{lim}-values chosen are a factor of about three higher than expected for unstirred solutions. Their better fit, however, is assumed to be due to the disturbencies introduced in terminating the immersion experiments. These disturbencies are also believed to make the experimental values for the exchange current somewhat too high.

Whereas the changes observed for the radioactive pickup with overvoltage and dissolution rate may seem well accounted for by the above model, the actual values obtained for the pickup are more difficult to explain. As shown above for the pickup at equilibrium, these values show that the stationary tracer concentration rapidly is reached within a whole surface layer, and this may indicate that the exchange, in one way or another, rapidly involves all surface atoms and not only those at steps and kinks. Further work is needed to clarify this matter.

ACKNOWLEDGEMENT

The authors are much indebted to Mrs. Toril Tønderum Eikeri and Miss Kari Storstrøm for technical assistance, to various members of the staff at the Central Institute for Industrial Research for valuable discussions, and to the U.S. Department of Army, European Research Office, for financial support.

REFERENCES

1. M. Haissinsky, J. Chim. Phys. 47 (1950) 957; M. Haissinsky, M. Cottin, and B.J. Varjabédian, ibid. 45 (1948) 212.
2. H. Gerischer and W. Vielstich, Z. Elektrochem. 56 (1952) 380.
3. H. Gerischer and R.P. Tischer, Z. Elektrochem. 58 (1954) 819.
4. C.V. King and N.E. McKinney, Can. J. Chem. 37 (1959) 205.
5. G.T. Miller Jr. and K.R. Lawless, J. Electrochem. Soc. 106 (1959) 854.
6. T. Hurlen, Acta Chem. Scand. 15 (1961) 1246.
7. T. Hurlen, Acta Chem. Scand. 15 (1961) 1239.
8. T. Hurlen, Acta Chem. Scand. 15 (1961) 615.
9. E. Mattsson and J.O'M. Bockris, Trans. Faraday Soc. 55 (1959) 1586.
10. J. O'M.Bockris and M. Enyo, Trans. Faraday Soc. 58 (1962) 1187.
11. T. Hurlen, Acta Chem. Scand. 15 (1961) 630.
12. T. Hurlen, Electrochim. Acta 7 (1962) 653.

FIGURES

Fig. 1. Stationary pickup and overvoltage for copper in the applied solutions at cupric concentrations of 0.001 M (closed circles), 0.01 M (open circles), and 0.1 M (centred circles).

Fig. 2. Stationary pickup and dissolution rate for copper in the applied solutions at cupric concentrations of 0.001, 0.01, and 0.1 M.

Fig. 3. Exchange current versus reversible potential for copper in the applied solutions.

Fig. 4. Experimental polarization points and theoretical polarization curves for copper in 0.1 N H_2SO_4 + 0.001 M $CuSO_4$ + x M $Fe_2(SO_4)_3$.

Fig. 5. Experimental polarization points and theoretical polarization curves for copper in (a) 0.1 N H_2SO_4 + 0.01 M $CuSO_4$ + x M $Fe_2(SO_4)_3$ and (b) 0.1 N H_2SO_4 + 0.1 M $CuSO_4$ + x M $Fe_2(SO_4)_3$.

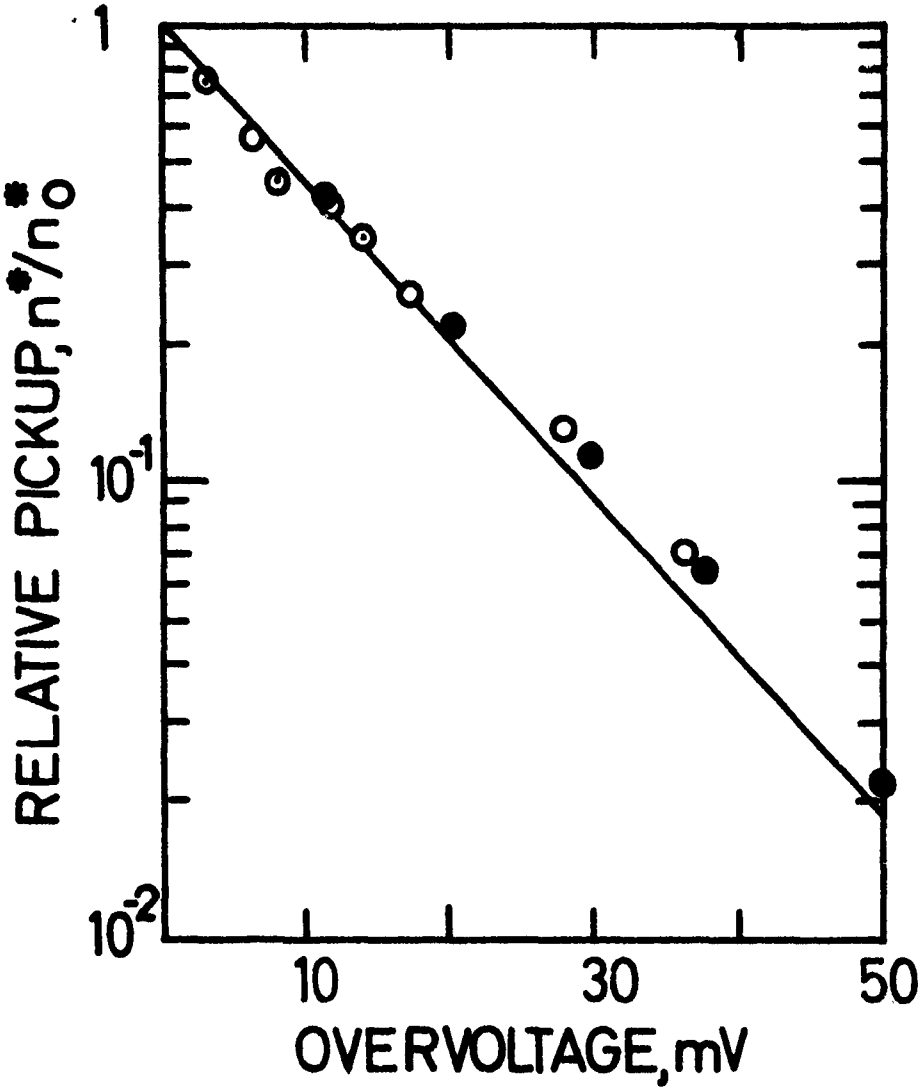

FIG.1.

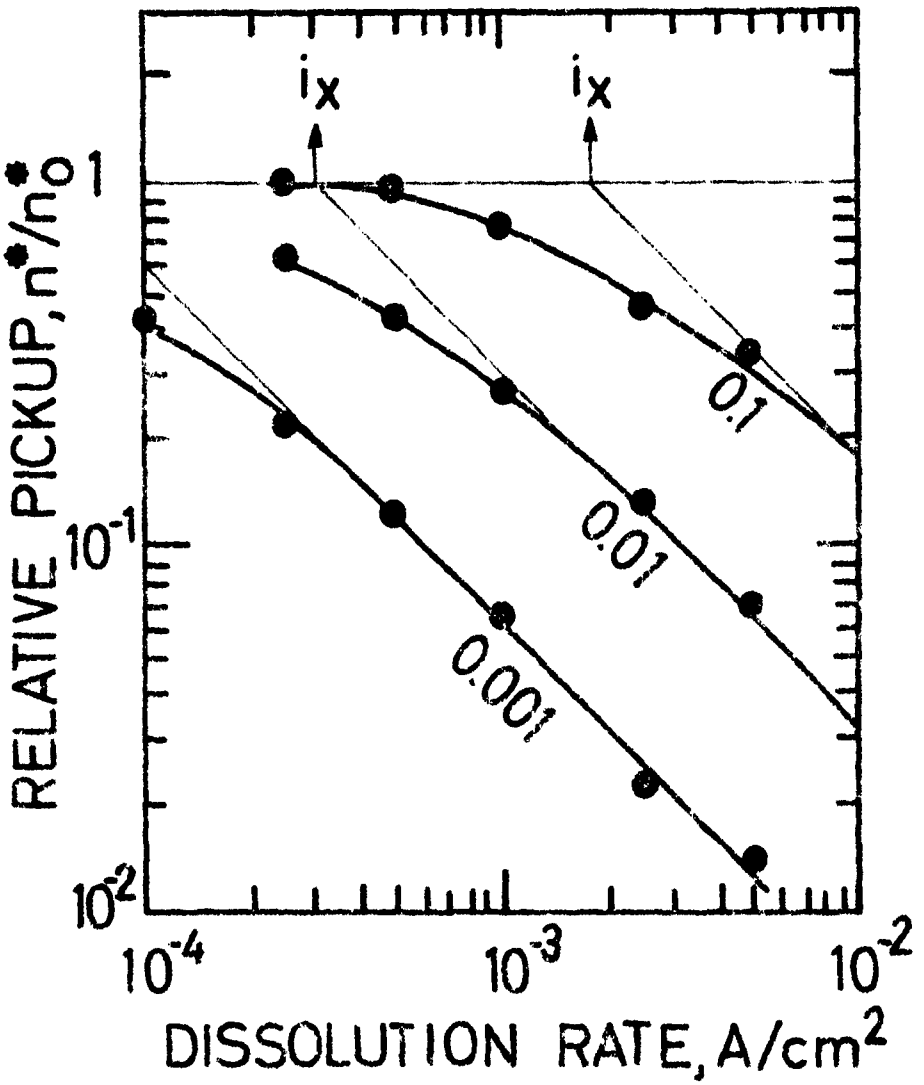
ix
ix
1
10^{-1}
10^{-2}
RELATIVE PICKUP, n^*/n_o^*
0.1
0.01
0.001
10^{-4}
10^{-3}
10^{-2}
DISSOLUTION RATE, A/cm^2

FIG. 2.

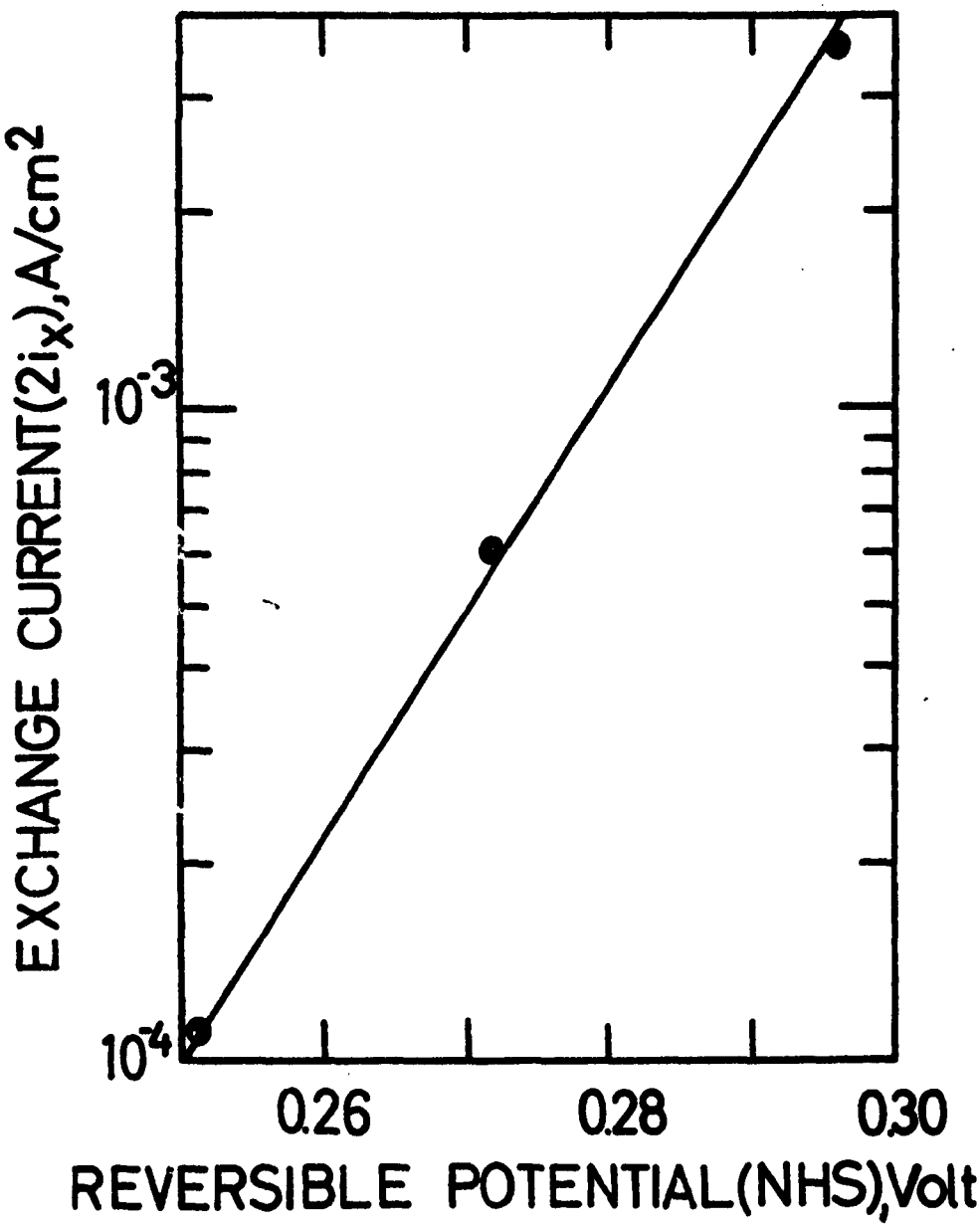
EXCHANGE CURRENT($2i_x$), A/cm^2
10^{-3}
10^{-4}
0.26
0.28
0.30
REVERSIBLE POTENTIAL(NHS), Volt

FIG.3.

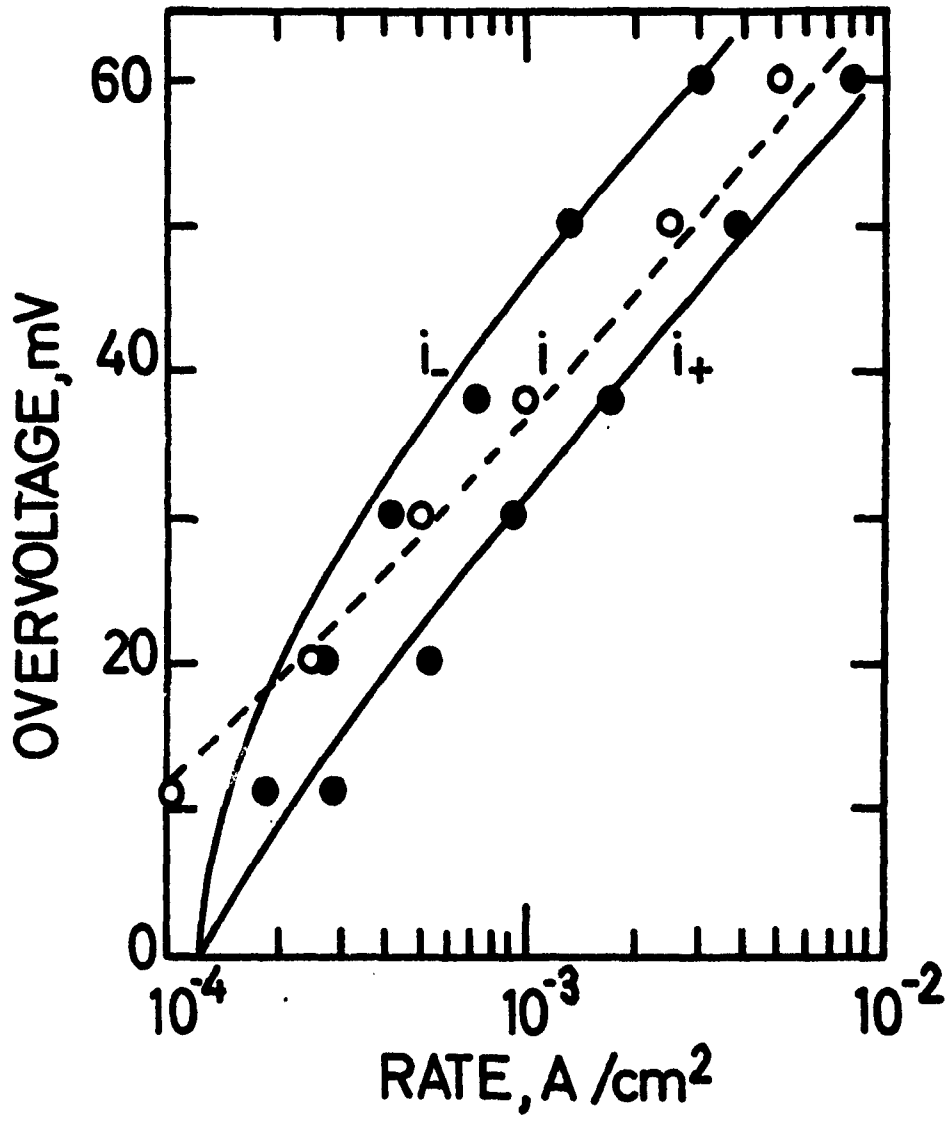

FIG.4.

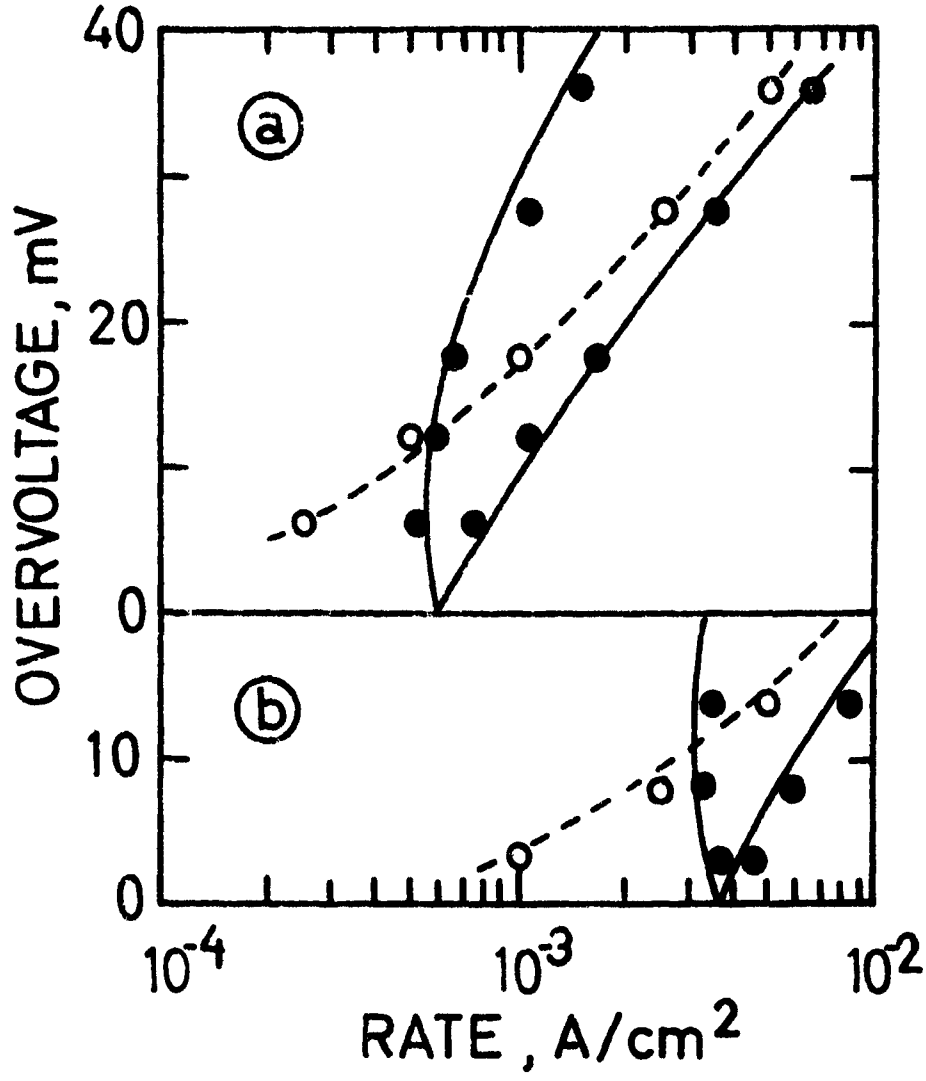

FIG. 5.

SI Publ. No. 390
Proj. No. 62 01 01

Special Scientific Report No. 2
Contract No. DA-91-591-EUC-2077

ANODIC BEHAVIOUR OF IRON IN ALKALINE SOLUTIONS

Tor Hurlen

December 1962

The research reported in this document has been made possible through the support and sponsorship of the U.S. Department of Army, through its European Research Office.

Central Institute for Industrial Research
Blindern, Oslo, Norway

St. 3628

ANODIC BEHAVIOUR OF IRON IN ALKALINE SOLUTIONS

Tor Hurlen

CENTRAL INSTITUTE FOR INDUSTRIAL RESEARCH
BLINDERN, OSLO, NORWAY

ABSTRACT

Galvanostatic experiments are made on iron electrodes in hydrogen poor and hydrogen saturated alkaline solutions at 20 °C. Emphasis is on the active behaviour of iron, but attention is paid also to its passivation.

The mechanism of the anodic dissolution of active iron is found to be the same in alkaline as in acid solutions. It is characterized by the dissolution reaction showing a first-order hydroxyl ion dependence and a V/ln i slope of RT/2F. The hydrogen electrode on active iron is found to have a pH-independent cathodic reaction of slope - 2RT/F and a second-order hydroxyl ion dependent anodic reaction of slope 2RT/3F (when activation controlled). The passivation curves show clear inflections in the vicinity of the reversible FeO/Fe_2O_3 and Fe_3O_4/Fe_2O_3 potentials.

A special discussion is given of the active dissolution reaction on the basis both of the present and of previous results.

St. 3628

1.0 INTRODUCTION

It is now well known that the dissolution[1-8] and the deposition[4-6] of iron at active iron electrodes in aqueous solutions are kinetically affected by the pH (or rather the pOH) in a way which corresponds to a catalytic interaction of hydroxyl ions. Discrepancies exist, however, as to the magnitude (stoichiometry) and the mechanism of this effect, and various opinions are also otherwise held as to the mechanism of the iron electrode reactions (see below).

So far, the dissolution of active iron and its pH dependence have mainly been studied in acid solutions, while most work on iron in alkaline solutions have concerned its passivation. This work clearly shows, however, that data are obtainable for the active dissolution reaction also in the latter type of solutions[1,9,10], and it is the scope of the present work to provide and discuss such data for a further elucidation of the reaction mechanism of the active iron electrode. Some attention is moreover paid to the hydrogen electrode reactions on iron and to the passivation of iron in alkaline solutions.

2.0 PREVIOUS WORK

The mentioned effect of pH was probably first pointed out by Kabanov, Burstein, and Frumkin[1]. By extrapolation of polarization data for the dissolution of active iron in an acid (1 N HCl) and in an alkaline (2 N NaOH) solution, they found that the dissolution at equal potentials proceeds ca. 10^{14} times as fast in the latter as in the former case (see especially Fig. 5 of Ref. 1). This was originally taken as an indication of the dissolution mechanism being widely different in acids and in alkalies. It could just as well mean, however, that one and the same mechanism is operating in these cases, and that this mechanism includes a first-order catalytic interaction of hydroxyl ions.

The latter interpretation is supported by more recent results which show that both the anodic dissolution[2-8] and the cathodic deposition[4-6] of iron in acid colutions are directly affected by the pH very nearly as prescribed. This behaviour was first observed by Bonhoeffer and Heusler[2] (dissolution) and by Hoar and Hurlen[4] (dissolution and deposition). The former authors, however, got an experimental value of about 1.5 for the hydroxyl ion exponent and assumed its correct value to be 2, whereas the latter authors got a value closer to 1. Subsequent work[5-7] may seem to support this first-order value, which further has been shown to be in accordance with the well known variation with pH of the corrosion potential of iron in acid solutions[6,11].

There was earlier some doubt whether the observed effect of pH was due to a stimulation by hydroxyl ions or to an inhibition by hydrogen ions[2]. The former may now seem largely accepted[1-8,12], however, but mechanisms have also been proposed in which such a distinction is immaterial[6,7]. Strong support for hydroxyl ions being the responsible species comes from studies on the effect of temperature on the iron electrode reactions in an acid solution[13]. In that solution, pH does not change very much with temperature, but pOH does (due to variations in the dissociation constant of water), and it has been found necessary to take this into account to have reasonable values for the mean standard heat and entropy of activation[14] of the iron electrode (see also Ref. 5).

Also the potential dependence of the active iron electrode reactions is subject to some controversies. This especially applies to deposition, in which case large uncertainties often are attached both to the rate ascribed to the reaction, and to the pH at which it is assumed to occur[5,6]. Bockris et al.[6] have tried to correct for pH-changes at the electrode surface, and have thereby introduced some very large corrections to their short-time polarization data. Corrections of that magnitude, however, are easily seen to be inapplicable to the long-time polarization data of Hurlen[5]. There further are data[4,5] indicating that the relative rates of hydrogen evolution and iron deposition initially varies with time, and that a steady ratio sometimes is obtained first after a time of the order of minutes. This obviously renders the interpretation of short-time data on the iron deposition reaction rather difficult. What we here strongly need is some sober long-time experiments on the effect of stirring (e.g. rotating disc) and of time on current efficiency and polarization behaviour.

In the case of dissolution, uncertainties of the above kind are of less importance, and discrepancies are smaller. The values given for the V/ln i slope under steady-state conditions mostly are from RT/2F to 2RT/3F, the one or the other of these extremes being the value believed in by various authors[1-6]. A clear distinction between these two values from polarization data at constant pH may sometimes be difficult, as the range for such measurements often is rather limited. A clearer distinction should be possible through the shift of the polarization curve along the potential axis when going from acid to alkaline solutions, provided the active dissolution mechanism is the same in these two cases (see above). With a first-order hydroxyl ion interaction, the shift from pH 0 to pH 14 should be 0.406 and 0.542 in the two respective cases at 20 °C. This gives a rather conclusive difference of 0.136 V between the two cases (a difference which further has to be doubled if the hydroxyl ion interaction should be second order). Tested in this way, the results of Kabanov, Burstein, and Frumkin[1] and also those of the present work

(see below) are strongly in favour of the lowest of the two Tafel slope values and of the first-order value for the hydroxyl ion exponent. The results summarized by Gerischer[9] (Fig. 5 of his paper) and the recent results of Nagayama and Cohen[15] (Fig. 2 of their paper) give further indications in the same direction.

Tafel lines, which on this basis are to be expected for the dissolution of active iron in alkaline solutions from previous results in acid solutions[5], are stipulated in Fig. 1. In the same diagram is further given the Tafel line previously obtained by the author[5] for the pH-independent evolution of hydrogen from water molecules at iron electrodes of exactly the same quality as in the present work, and the position of the reversible point for the 1 atm. hydrogen electrode on this material at some pH-values is shown. These data clearly indicate that active iron may act as a hydrogen electrode at pH-values above 12 (as previously discussed[11]). The determination of proper data for the iron dissolution reaction in alkaline solutions will thereby certainly be impeded, unless the "hydrogen pressure" at the electrode can be kept low enough to make the anodic hydrogen oxidation reaction negligibly slow. In the present work, attention is paid to this matter, and experiments have been made both with hydrogen saturated solutions in nearly closed cells and with hydrogen poor solutions in open cells.

3.0 EXPERIMENTAL WORK

All experiments have been performed galvanostatically in a thermostated room at about 20 °C. No stirring was applied neither in the closed nor in the open cells used (see below). The current was supplied from an assembly of four 12 V accumulators connected in series. It was controlled by a number of variable resistances and read on a calibrated Avo-meter. Potential measurements were carried out conventionally by means of a saturated calomel electrode and a Radiometer compensator in an essentialle currentless Luggin-capillary containing circuit. The calomel electrode has been ascribed a standard hydrogen scale potential of 0.248 V at the temperature concerned[15], and all potentials have accordingly been referred to the standard hydrogen scale. No attempts have been made to correct for possible liquid junction potentials between the test solutions and the saturated potassium chloride solution of the reference half-cell.

Electrodes of iron with 0.03 % C, 0.01 % Si, 0.19 % Mn, 0.027 % P, and 0.030 % S were used partly in the form of circular sheets of diameter 4.5 cm (closed cell experiments) and partly in the form of rectangular sheets of 1.5 x 2 cm with a small shaft for suspension (open cell experiments). The sheet thickness was about 0.5 mm. After fabrication, the electrodes were vacuum annealed for one hour at 700 °C, polished with emery paper, degreased with chloroform, etched in dilute nitric acid, rinsed in running water and distilled water, dried with acetone, and stored in a desiccator. Prior to use, they were re-etched for at least twenty minutes in 1 N hydrochloric acid and rapidly washed with distilled water immediately before being exposed to the test solution. For the closed cell experiments, this re-etching was performed in the cell itself. After immersion, the test electrodes further were cathodically activated at current densities from 50 to 100 $\mu A/cm^2$ until the cathodic polarization was essentially what to be expected (from Fig. 1) for hydrogen evolution on active iron.

Solutions were prepared from A.R. quality potassium hydroxide, sodium hydroxide, and potassium chloride in water distilled from a

rather pure fresh water, and they were stored for as short time as possible in hard polythene containers. Solutions for closed cell experiments were further pre-saturated with and stored under purified hydrogen.

Closed cell experiments were performed with the cell previously described[5]. In brief, this is a cylindrical Pyrex cell with tubes for the ingress and egress of liquid and gass, circular electrodes (of iron in the present case) forming its end walls. It holds about 200 ml electrolyte, which is exposed to the atmosphere in two capillaries only.

Open cell experiments were simply performed in a 500 ml Pyrex beaker with electrolyte connections to a 100 ml beaker in which an auxiliary platinum electrode was placed, and with a Luggin capillary tube leading to the reference electrode. The electrolyte connections were arranged so as to favour a symmetric distribution of the applied current to both sides of the test electrode. The iron test electrode was completely immersed in the test solution and was suspended by means of a Pyrex tube into which its shaft and metallic connections to the battery and potentiometer circuits were moulded by means of an Araldite.

4.0 RESULTS AND INTERPRETATIONS

The cathodic polarization data obtained in connection with the activation of iron electrodes confirmed that the hydrogen evolution reaction on active iron in alkaline solutions at 20 °C essentially obeys the pH-independent Tafel line given in Fig. 1.

In Fig. 2, examples are given of potential/time curves obtained for iron in open cell experiments at zero current after cathodic activation for one hour at 10^{-4} A/cm^2. These curves apply to pure sodium hydroxide solutions of various molalities, and they clearly show that the conditions for studies on the anodic dissolution of active iron are best at medium hydroxide concentrations (0.1 - 0.3 M). At lower concentrations, passivation phenomena too easily come in. At higher concentrations, a steady corrosion potential is too slowly approached, possibly because of an increased interference from hydrogen (as discussed above).

In Fig. 3, examples are given of potential/time curves obtained for iron at various applied anodic current densities in the open cell. These curves apply to a 0.3 M sodium hydroxide solution. In these cases, the anodic current was switched on about half an hour after a cathodic activation for one hour at 10^{-4} A/cm^2 (i.e. first after the establishment of a steady corrosion potential). Quite similar curves were obtained in 0.1 M and to some extent also in 1 and 3 M sodium hydroxide solutions, all showing four levels of the types notified by A, B, C, and D in Fig. 3. In the two latter solutions, however, a steady corrosion potential was difficult to obtain prior to application of anodic currents, and the "A-level" became less defined and clearly dependent on the potential reached before the anodic current was switched on. Also this may possibly be due to an interference by hydrogen as discussed above.

In Fig. 4, examples are given of potential/time curves obtained for iron at various applied anodic current densities in the closed cell. These curves apply to hydrogen pre-saturated sodium hydroxide solutions of 0.3, 1, and 3 M, respectively, the latter two being in

addition 1 M in potassium chloride. In all these cases, the anodic current was applied immediately after cathodic activation for two hours at 5×10^{-5} A/cm^2 by simply adjusting and reversing the current. In the 3 M sodium hydroxide solution, the cathodic pre-treatment applied did not give a proper activation of the iron surface, as judged from the cathodic potentials observed. This impedes the interpretation especially of the A-level potentials obtained in that solution.

Active Iron

The A-level obviously is nearest to representing the steady-state behaviour of active iron. It thus is of major interest for the elucidation aimed at in the present work.

In Fig. 5, representative data for the polarization at this level are presented in a Tafel diagram. Open and closed cell data are there given by open and closed points, respectively, and are seen to differ from each other, except at the lowest hydroxyl ion concentration concerned (0.1 M). This is qualitatively in accordance with the differences to be expected for active iron anodes in hydrogen poor and in hydrogen saturated solutions from the predictions in Fig. 1, and it strongly suggests that we here have data both for the iron dissolution reaction and for the hydrogen oxidation reaction.

The solid Tafel lines in Fig. 5 are thus believed to represent the anodic dissolution of active iron. These lines are drawn with a slope of 2.303 RT/2F, which is in accordance with the predictions in Fig. 1. Also their position in the diagram (and their shift with pH) are in reasonable agreement with these predictions. This strongly supports the view that the dissolution mechanism of active iron is the same in alkaline as in acid solutions, and that this mechanism is characterized by a V/ln i slope of RT/2F and by a first order hydroxyl ion interaction.

The stipulated anodic Tafel lines in Fig. 5 are similarly believed to represent the hydrogen oxidation reaction at active iron electrodes. This is supported by their points of intersection with the cathodic

hydrogen line giving reasonable values for the reversible potential of the hydrogen electrode in the respective solutions. The pH-independent cathodic hydrogen line in Fig. 5 is the same as the one in Fig. 1 and has a V/ln i slope of numerically 2RT/F. The anodic hydrogen lines are drawn with corresponding slopes of 2RT/3F, and this may seem to fit the experimental results reasonable well. The anodic hydrogen reaction is further seen to be second order in hydroxyl ion dependence.

Passive Iron

On its way from the active state (A) to oxygen evolution (D), the iron electrode in the present cases passes two states (B and C) which clearly show themselves by levels or inflections in the galvanostatic passivation curves. This is in accordance with previous results in alkaline[9, 10, 17] and nearly neutral[15] solutions, and it has been interpreted[10] as reflecting the formation of a primary passive layer of Fe_3O_4 (at B) and the transformation of this into a final composite layer of Fe_3O_4 and γ-Fe_2O_3 (at C).

The C-level potentials observed in the present work are in reasonable agreement with estimated values for the reversible Fe_3O_4/γ-Fe_2O_3 potential[10,17]. The C-level thus corresponds to the Flade potential for passivation of iron in acid solutions, a potential which shows itself by an inflection also in activation curves for passive iron. In this connection it is further interesting to note that passivated iron electrodes in alkaline solutions often stabilize at this potential when the anodic current is cut off (as exemplified by the stipulated curves in Fig. 3).

The B-level potentials observed in the present work are appreciably higher than the reversible Fe/Fe_3O_4 potential (-0.08 - 0.058 pH) which by Vetter[10] is assumed to represent the transition between activity and passivity for iron in alkaline solutions. They are much nearer to what may be estimated for a reversible $Fe(OH)_2/Fe(OH)_3$ or FeO/Fe_2O_3 potential[10, 18, 19]. This also applies to the active/passive transition observed by Nagayama and Cohen[15] in a nearly neutral solution and probably to the corresponding data of Heusler, Weil, and

Bonhoeffer[17] in alkaline solutions. In reproducing the latter data, Vetter[10] may seem to have given the transition potentials too low values. The observations made in the present work of a distinct overshoot in the potential at the initial part of the B-level (Figs. 3 and 4) and of a doubling of this level at high hydroxyl concentration (Fig. 4 C) may also be of importance in elucidating the processes occuring there. Except for noting this, no further discussion will here be given of this matter, as it is outside the main scope of the present work.

5.0 DISCUSSION

The results described and discussed above for the passivation of iron mainly are bi-products of the present work. In this discussion, therefore, we shall only consider the behaviour of active iron under essentially steady-state conditions.

In Fig. 6, a combined presentation is given of what is indicated by the present results in alkaline solutions and previous results in acid solutions (see Ref. 5 where further references are given) for the potential and pH dependence of the anodic dissolution reaction (solid lines) and the hydrogen reactions (dashed lines) at active iron electrodes (when the reactions are under activation control). The anodic hydrogen lines apply to a hydrogen pressure of 1 atm, and all lines apply to a temperature of 20 °C. In the same diagram is further shown the position of the reversible hydrogen point (closed circles) and of the iron corrosion point (open circles) at various pH-values (when the hydrogen pressure is 1 atm and there is a pure hydrogen evolution type of corrosion). What by the latter points is shown for the effect of pH on the corrosion rate and the corrosion potential of active iron, agrees with what has previously been deduced by the author and shown to be in accordance with old knowledge[11].

The Iron Electrode.

The presentation given in Fig. 6 of the potential and pH dependence of the iron dissolution reaction is mainly based on experimental results in the pH-regions 0-4 (Refs. 1-6) and 13-14 (present work and Ref. 1). In the intermediate pH-region 4-13 there obviously are greater difficulties in obtaining proper data of this kind, partly because of stronger demands for pH-control and partly because of stronger limitations imposed by passivation. Of the few pertinent data in this pH-region, those obtained by Nagayama and Cohen[15] at a pH of about 8 and a temperature of about 20 °C may be noted. The anodic polarization curve given by these authors for active iron (when not

too close to the active/passive transition) is in reasonable agreement with Fig. 6. The same may seem to apply also to results of Heusler, Weil, and Bonhoeffer[17] at a pH of about 9, but the comparison is here impeded by their data applying to 50 °C. The work of Christiansen et al.[7] also concerns this intermediate pH-range, but the use of their data is even more impeded by these not applying to steady-state conditions.

Altogether, there clearly are strong enough indications that the steady-state dissolution occurs by one and the same mechanism in acids as in alkalies, and that this mechanism involves a first-order hydroxyl ion interaction and gives rise to a V/ln i slope of RT/2F. The correctness of this is perhaps most strongly supported by the shift observed for the Tafel line when going from acid to alkaline solutions (see the above discussion of previous work).

As previously shown by the author [5,14] and by Hoar[20] and Bockris et al.[6] (and more generally also by Parsons[21] and Vetter[10]), the kinetic reaction equation representing the above data must be:

$$2\,Fe + OH^- = 2\,Fe^{2+} + OH^- + 4e^-$$

or

$$2\,Fe + OH^- = Fe(OH)^+ + Fe^{2+} + 4e^-$$

An explanation of this behaviour has already been suggested by the author[14] on the basis of the dislocation theory of crystal growth and dissolution[22]. By this explanation, a chain reaction mechanism is favoured in which kinks (kossel sites) are formed by a pH-dependent and direct dissolution of single atoms from crystal steps (initiation reaction) and act as chain carriers for a pH-independent and direct dissolution of single atoms at kinks (propagation reaction) until they disappear (termination reaction). Such a mechanism may seem to be in accordance with the observed kinetics.

For thermodynamic reasons, the mechanism of cathodic deposition of iron from ferrous species must on the above basis also be the same

in alkaline as in acid solutions. This is of interest in showing that the proper reactants for this electrode reaction are those of the right hand side of the above equations and not the more abundant ferroate anion.

The Hydrogen Electrode.

The hydrogen electrode on active iron clearly changes from involving hydrogen ions in acid solutions to involving water and hydroxyl ions in alkaline solutions. This makes the exchange current to decrease with increasing pH in acid solutions and to increase in alkaline solutions. The transition may seem to occur slightly to the acid side of pH 7 (see Fig. 6).

In acid solutions, the hydrogen evolution reaction is first order in hydrogen ion dependence and has a V/ln i slope of $-2RT/F$. To the authors knowledge, direct data on the reverse hydrogen oxidation reaction on iron in acid solutions are unobtainable. The line given for this reaction in Fig. 6 has merely been drawn through the reversible points and need not be truly representative. It is equally possible that this reaction should be represented by pH-dependent lines of the same slope as found in alkaline solutions (see below).

In alkaline solutions, the hydrogen avolution reaction is independent of pH and has a V/ln i slope of $-2RT/F$ (i.e. the same as in acid solutions). The hydrogen oxidation reaction is here second order in hydroxyl ion dependence and has a slope of $2RT/3F$. This compares well with what is to be expected for a Volmer-Heyrowsky mechanism with Volmer control in case of low coverage of the electrode surface by adsorbed hydrogen atoms and Heyrowsky control in case of high coverage[10].

ACKNOWLEDGEMENT

The author is much indebted to siv.ing. B. Haraldsen for introductory measurements, to Mrs. T. Tønderum Eikeri and Miss K. Storstrøm for technical assistance, to various members of the staff at the Central Institute for Industrial Research for helpful discussions, and to the U.S. Department of Army, European Research Office, for financial support.

REFERENCES.

1. B. Kabanov, R. Burstein, and A.N. Frumkin, Discuss. Faraday Soc. 1 (1947) 259.

2. K.F. Bonhoeffer and K.E. Heusler, Z. physik. Chem. N.F. 8 (1956) 390; Z. Elektrochem. 61 (1957) 122.

3. K.E. Heusler, Z. Elektrochem. 62 (1958) 582.

4. T.P. Hoar and T. Hurlen, unpublished work (Cambridge 1956); T. Hurlen, Tek. Ukeblad 105 (1958) 101 and 119.

5. T. Hurlen, Acta Chem. Scand. 14 (1960) 1533.

6. J. O'M. Bockris, D. Drazic, and A.R. Despic, Electrochim. Acta 4 (1961) 325; J. O'M. Bockris and D. Drazic, Electrocim. Acta 7 (1962) 293.

7. K.A. Christiansen, H. Høeg, K. Michelsen, G. Nielsen, and H. Nord, Acta Chem. Scand. 15 (1961) 300.

8. H. Fischer and H. Yamaoka, Chem. Ber. 94 (1961) 1477; K.J. Vetter and G. Klein, Z. physik. Chem. N.F. 31 (1962) 405; older references in Ref. 5.

9. H. Gerischer, Angew. Chem. 70 (1958) 285.

10. K.J. Vetter, Elektrochemische Kinetic, Springer, Berlin/ Gøttingen/Heidelberg (1961).

11. T. Hurlen, Acta Chem. Scand. 14 (1960) 1555.

12. T. Hurlen, Acta Chem. Scand. 14 (1960) 1564.

13. H. Gerischer, Electrochim. Acta 2 (1960) 1.

14. T. Hurlen, Electrochim. Acta, in press.

15. M. Nagayama and M. Cohen, J. Electrochem Soc. 109 (1962) 781.

16. D.J. Ives and G.J. Janz, Reference Electrodes, Academic Press, New York/London (1961).

17. K.E. Heusler, K.G. Weil, and K.F. Bonhoeffer, Z. physik.Chem. N.F. 15 (1958) 149.

18. W.M. Latimer, Oxidation Potentials (2nd ed.), Prentice-Hall, New York (1952).

19. M.J.N. Pourbaix, Thermodynamics of Dilute Aqueous Solutions, Arnold, London (1949).

20. T.P. Hoar, Modern Aspects of Electrochemistry No. 2 (Ed. J.O'M. Bockris), Butterworths, London (1959), Chapter 4.

21. R. Parsons, Trans. Faraday Soc. 47 (1951) 1332.

22. W.K. Burton, N. Cabrera, and F.C. Frank, Phil. Trans. Royal Soc. (London) A 243 (1951) 299.

FIGURES

Fig. 1. Anticipated Tafel diagram for the anodic dissolution reaction (solid lines), the hydrogen evolution reaction (dashed line), and the reversible hydrogen electrode (points) at active iron electrodes in alkaline solutions of various pH and 20 °C. (Anticipated from data in acid solutions[5]).

Fig. 2. Potential/time curves for cathodically activated (1 h at 10^{-4} A/cm^2) iron at zero applied current in sodium hydroxide solutions of various molalities (0.03-3 M). Open cell, 20 °C.

Fig. 3. Anodic potential/time curves for iron in 0.3 M sodium hydroxide at various applied current densities (10-80 μA/cm^2) put on half an hour after a cathodic activation for one hour at 100 μA/cm^2. Open cell, 20 °C.

Fig. 4. Anodic potential/time curves for cathodically activated (2 h at 50 μA/cm^2) iron at various applied current densities (0-0.6 mA/cm^2) in hydrogen saturated solutions of (a) 0.3 M NaOH, (b) 1 M NaOH + 1 M KCl, and (c) 3 M NaOH + 1 M KCl. Closed cell, 20 °C.

Fig. 5. Tafel diagram presentation of polarization data for active iron in solutions of various sodium hydroxide molalities (0.1 - 3 M) from open cell (open points) and closed cell (closed points) experiments. 20 °C.

Fig. 6. Combined Tafel diagram for the iron dissolution reaction (solid lines) and the hydrogen reactions (dashed lines) at active iron electrodes in hydrogen saturated (1 atm) solutions of various pH (0-14), showing also the effect of pH on the reversible hydrogen electrode (closed points) and on the mixed iron/hydrogen corrosion electrode (open points). 20 °C.

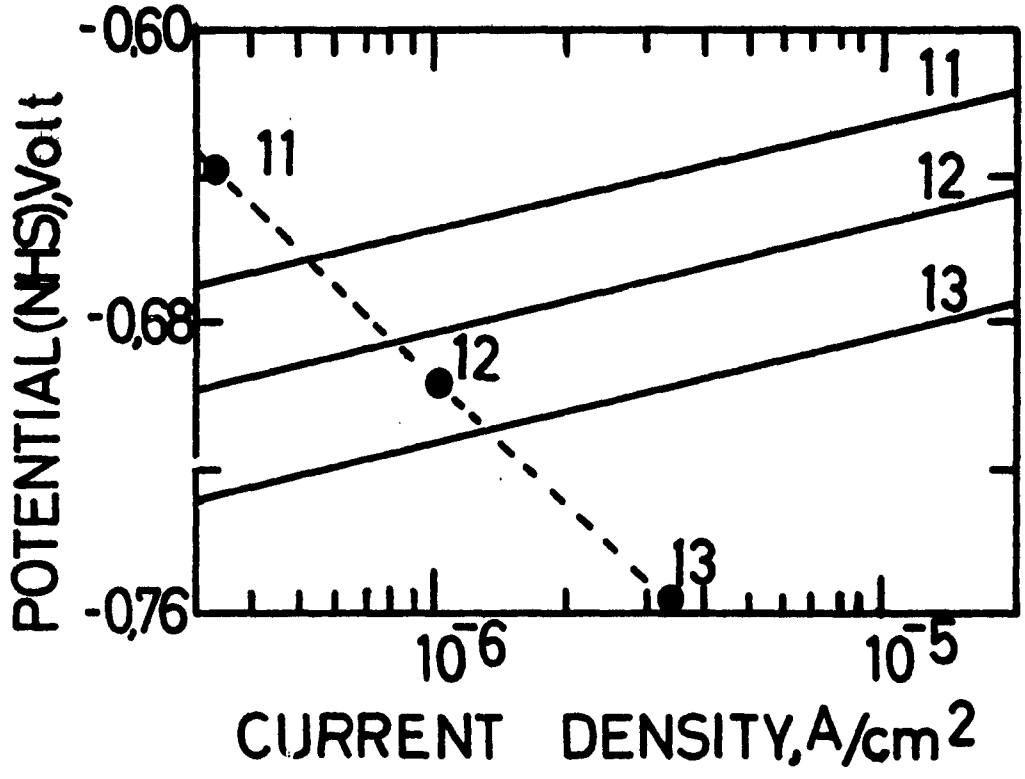
-0,60
-0,68
-0,76
POTENTIAL(NHS),Volt
11
12
13
11
12
13
10^{-6}
10^{-5}
CURRENT DENSITY, A/cm 2

FIG.1

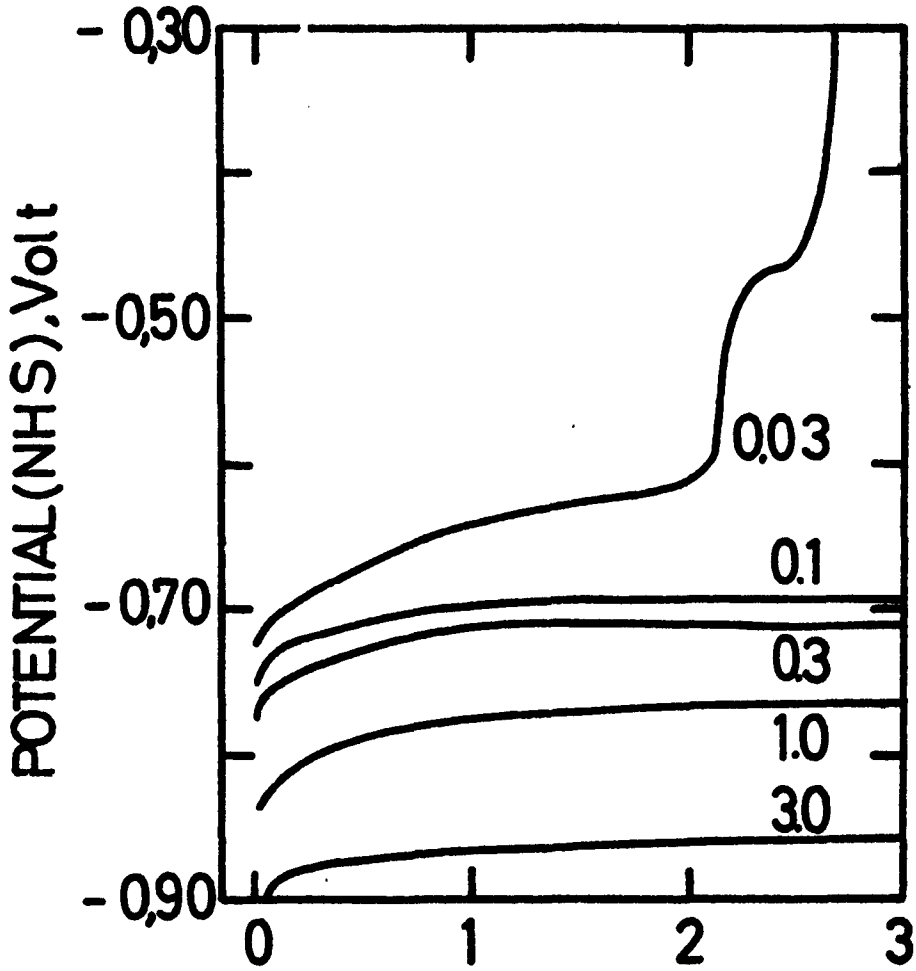
- 0,30
-0,50
-0,70
- 0,90
POTENTIAL (NHS), Volt
0.03
0.1
0.3
1.0
3.0
0
1
2
3
TIME , hours

FIG. 2

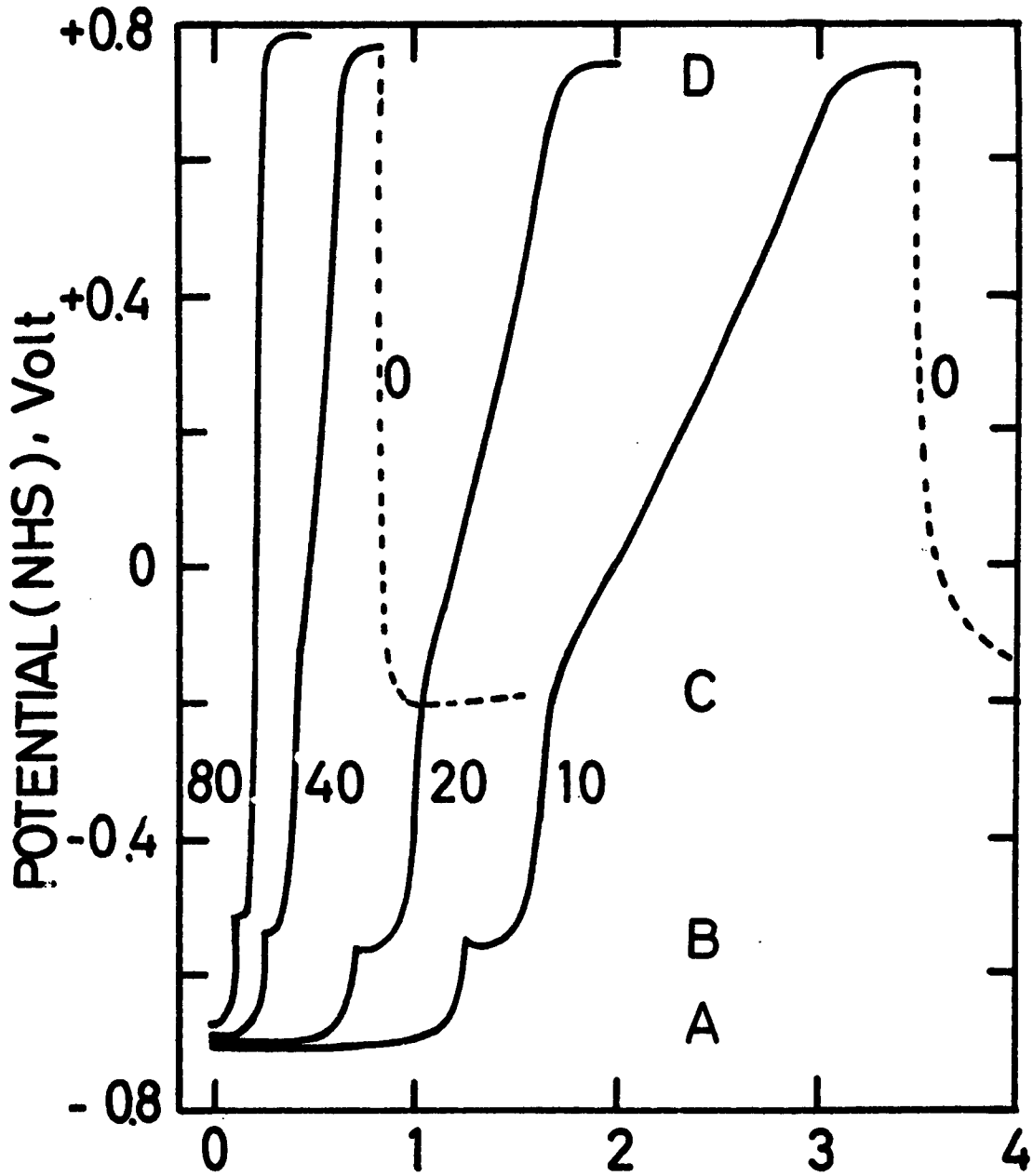
+0.8
+0.4
0
-0.4
-0.8
POTENTIAL (NHS), Volt
0
1
2
3
4
TIME, hours
80
40
20
10
0
0
A
B
C
D

FIG. 3

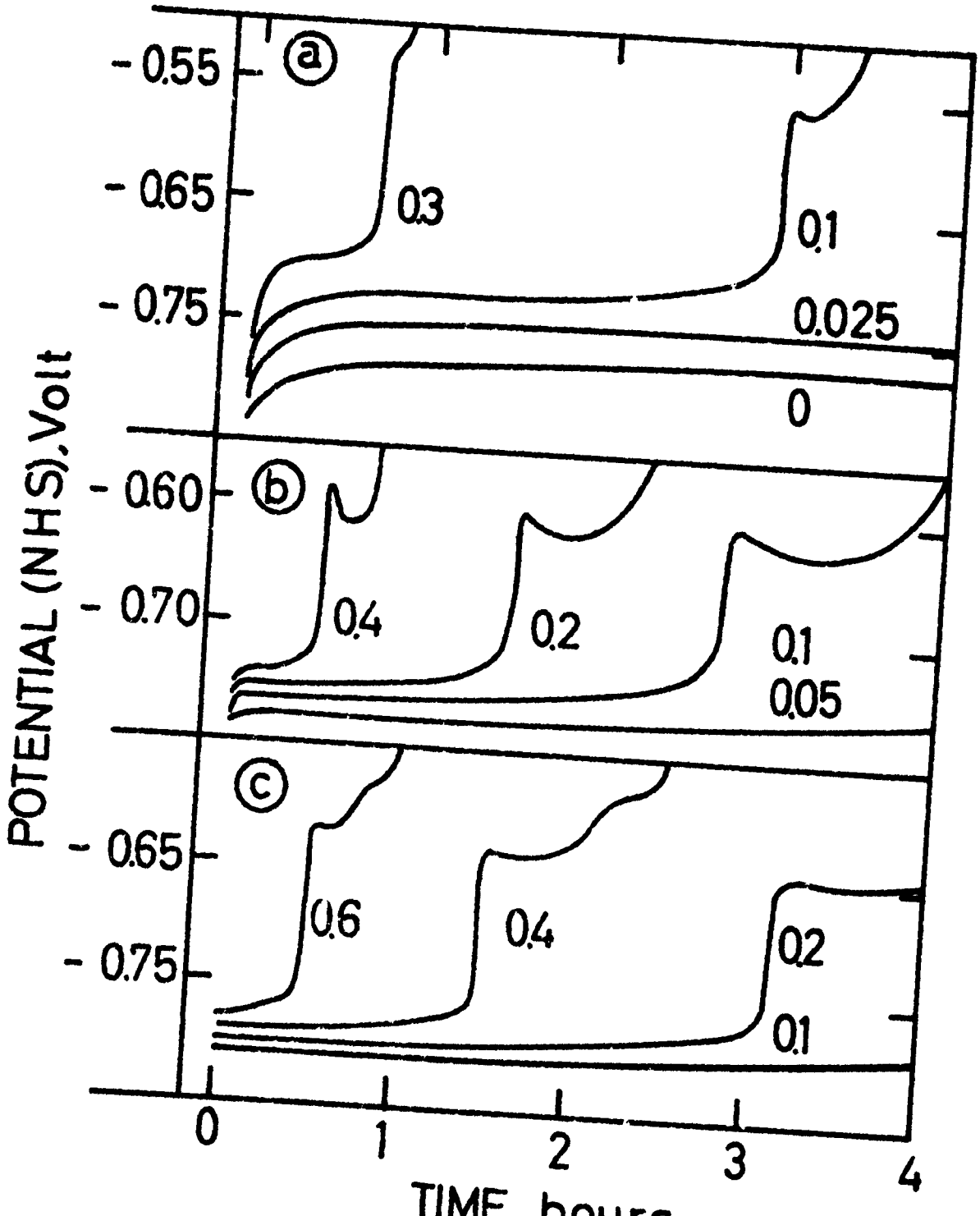
- 0.55
- 0.65
- 0.75
- 0.60
- 0.70
- 0.65
- 0.75
POTENTIAL (NHS), Volt
a
b
c
0.3
0.1
0.025
0
0.4
0.2
0.1
0.05
0.6
0.4
0.2
0.1
0
1
2
3
4
TIME, hours

FIG.4

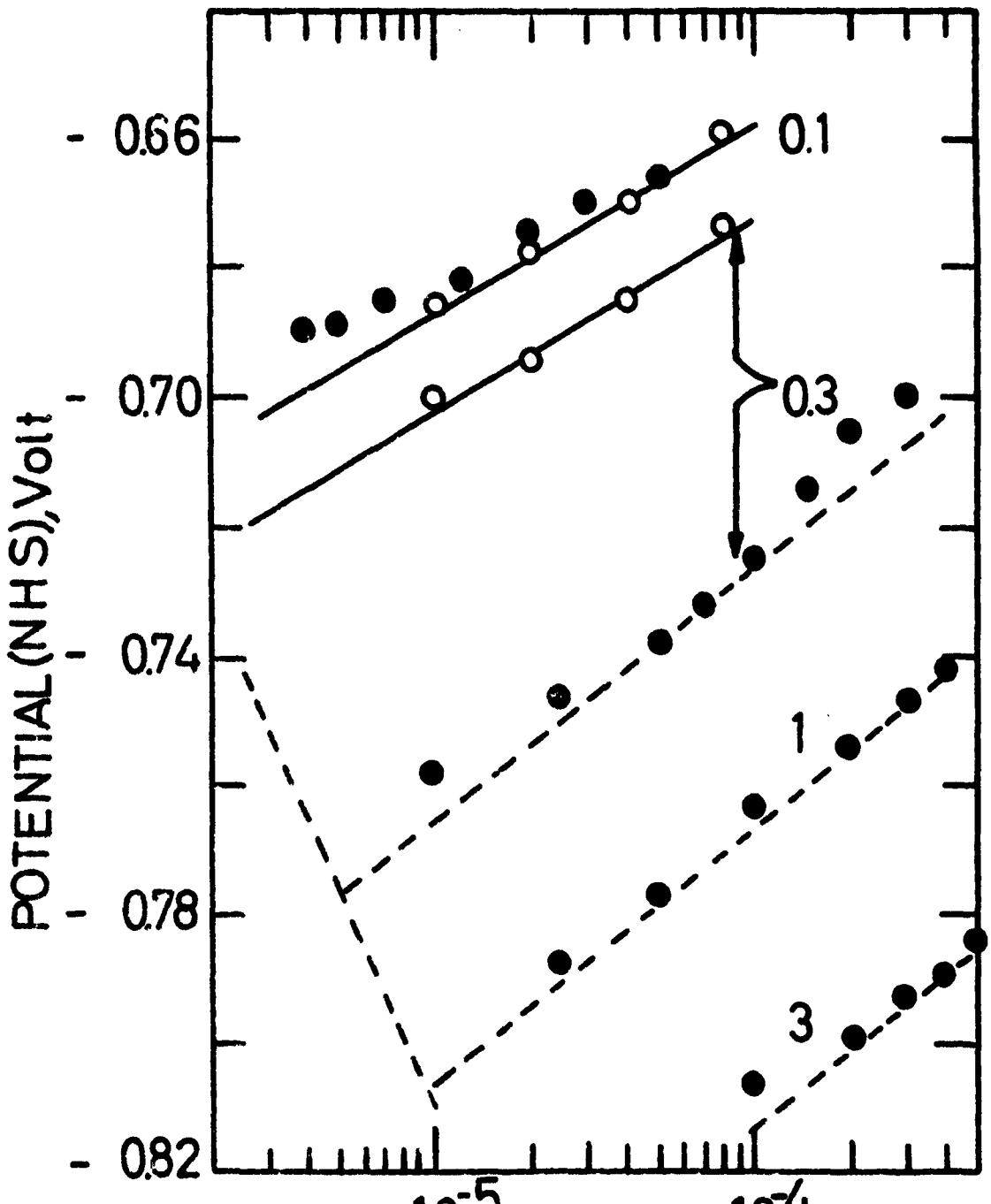
- 0.66
- 0.70
- 0.74
- 0.78
- 0.82
POTENTIAL (NHS), Volt
0.1
0.3
1
3
10^{-5}
10^{-4}
CURRENT DENSITY, A/cm^2

FIG.5

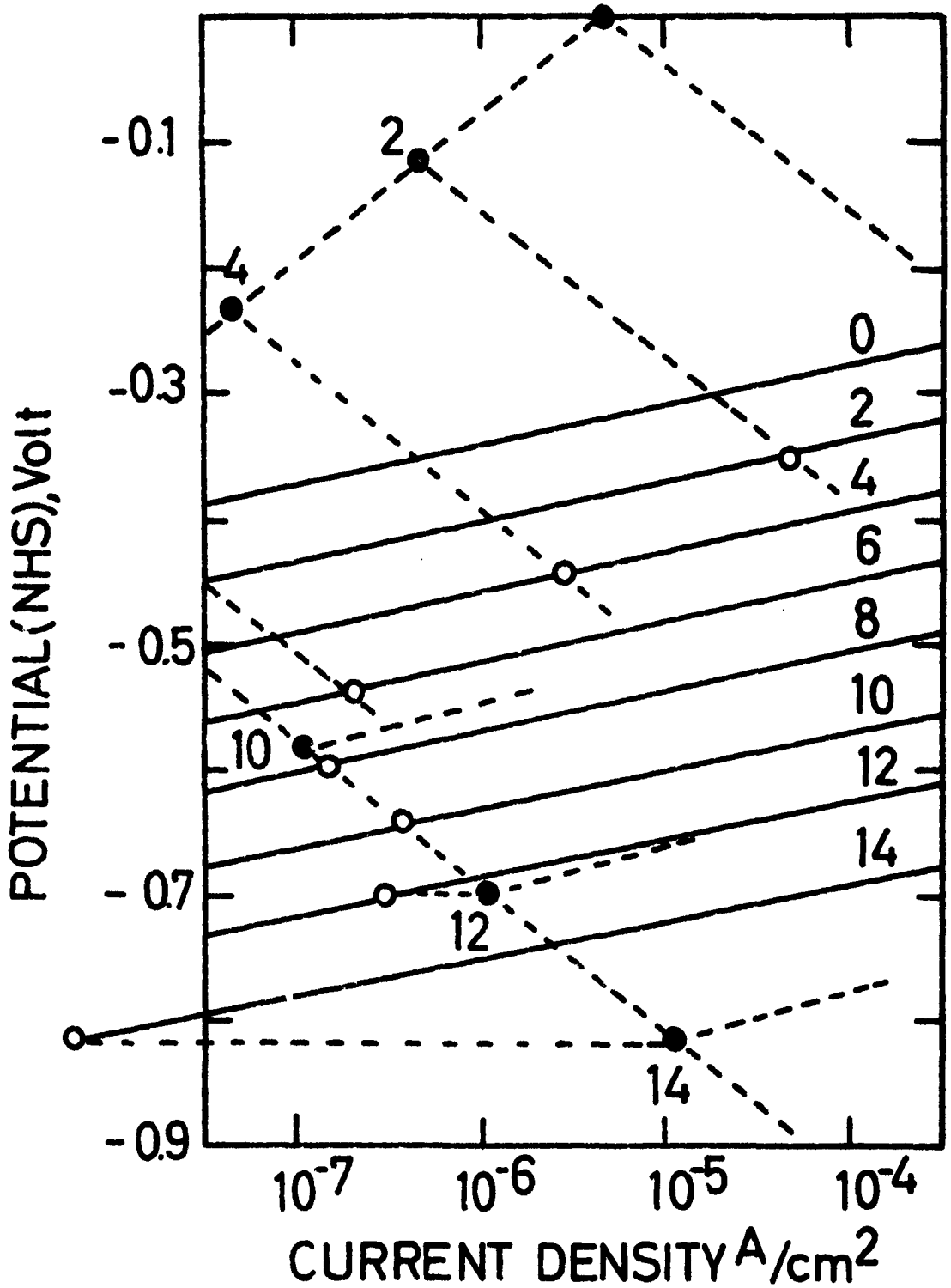
-0.1
-0.3
-0.5
-0.7
-0.9
POTENTIAL(NHS), Volt
2
4
10
12
14
0
2
4
6
8
10
12
14
10^{-7}
10^{-6}
10^{-5}
10^{-4}
CURRENT DENSITY A/cm^2

FIG.6

SI Publ. No. 370
Proj. No. 62 01 01

Special Scientific Report No. 1
Contract No. DA-91-591-EUC-2077

KINETICS OF METAL/METALION ELECTRODES
Iron, Copper, Zinc

Tor Hurlen

May 1962

The research reported in this document has been made possible through the support and sponsorship of the U.S. Department of Army, through its European Research Office.

Central Institute for Industrial Research
Blindern, Oslo, Norway

St. 3343/0

KINETICS OF METAL/METALION ELECTRODES
Iron, Copper, Zinc

Tor Hurlen
Central Institute for Industrial Research
Blindern, Oslo, Norway

ABSTRACT

The transition-state theory of activation controlled electrode reactions is discussed and is shown to give a proper description without implications of absolute potentials. This method of treatment is applied to steady-state data on dissolution and deposition of iron, copper, and zinc. Both steady-state and transient data on these (and other) solid metal/metalion electrodes are further discussed on the basis of crystal growth and dissolution theories, and comparisons are made to liquid metal/metalion electrodes.

For solid metal/metalion electrodes, a chain reaction mechanism is suggested that makes the transient superpolarization, the steady-state second-order kinetics, and the partial pH-dependence (Fe,Co) of such electrodes intelligible. The possibility of obtaining absolute electrode potentials by combining kinetic and thermodynamic data is considered.

1.0 INTRODUCTION

As part of a research programme on the kinetics of metal/metalion electrodes in aqueous solutions, the reactions of the Fe/Fe^{++}_{aq} electrode[1-4], the Cu/Cu^{++}_{aq} electrode[5-8], the Zn/Zn^{++}_{aq} electrode[9-11], and the complex $Cu/CuCl_x^{(x-1)-}$ electrode[12] have recently been studied under well comparable conditions by one and the same slow galvanostatic technique and also by other methods. The latter electrode has been shown to exhibit pure concentration polarization at 20 °C in unstirred solutions and even at stirring rates giving a five-fold increase of the limiting deposition current. Though concentration polarization to some extent also affects the reactions of the Cu/Cu^{++}_{aq} and the Zn/Zn^{++}_{aq} electrode in unstirred solutions (especially at temperatures above 20 °C), there are no great difficulties in determining the activation controlled behaviour of these electrodes (see especially Ref.[9]), nor of the Fe/Fe^{++}_{aq} electrode. In the papers referred to above, stationary-state data of this kind are given for the three divalent metal/metalion electrodes mentioned. Here we shall use these data as examples in discussing the reaction mechanism of such electrodes on the basis of fundamental theories of electrode kinetics and crystal growth.

In the first part of this paper, convenient transition-state equations for treating activation controlled electrode reactions are derived. In the second part, these equations are applied to the above divalent metal/metalion electrodes. In the third part, some further considerations are made from the point of view of crystal growth.

2.0 THE TRANSITION-STATE THEORY

In this chapter, we shall develop a convenient set of transition-state equations for the treatment of activation controlled electrode reactions under conditions of negligible potential differences outside the rigid part of the electrical double layer. These equations will thus apply to cases in which there is no specific adsorption at the electrode and a sufficient excess inert electrolyte is present.

For the mutually reverse anodic and cathodic reactions of an electrode with the kinetic unit equation (i.e. the equation which represents the reaction occurring for each act of the rate-determining step and also includes possible catalytic reactants):

$$\text{Red} = \text{Ox} + ne^- \qquad (1)$$

the absolute rate theory easily leads to the following rate expressions (assuming both the probability factor and the transition-state activity coefficient equal to unity):

$$i_+ = nF \frac{kT}{h} c_o^* \frac{(\text{Red})}{(\text{Red})_o} \exp\left(-\frac{\Delta G_{o,+}^*}{RT}\right) \exp\left(\frac{\alpha nF \Delta\phi}{RT}\right) \qquad (2a)$$

$$i_- = nF \frac{kT}{h} c_o^* \frac{(\text{Ox})}{(\text{Ox})_o} \exp\left(-\frac{\Delta G_{o,-}^*}{RT}\right) \exp\left(\frac{(\alpha-1)nF\Delta\phi}{RT}\right) \qquad (2b)$$

where c_o^* is the concentration in mole per unit area of the "activated complex" in the standard state chosen for it; (Red) and (Ox) are the mass action product of the anodic and cathodic reactants on whatever activity scale (or scales) one may choose; $(\text{Red})_o$ and $(\text{Ox})_o$ are the value of these products on the chosen scale (or scales) when each reactant is in the standard state chosen for it; $\Delta G_{o,+}^*$ and $\Delta G_{o,-}^*$ are the standard chemical energy of activation of the anodic and cathodic reaction, respectively; $\Delta\phi$ is the absolute potential difference between metal and solution; and the other symbols have their usual meaning.

This way of writing the rate equations deviates from the usual one[13,14] in the explicit mentioning of the standard states. This has the advantage of directly giving the rate equations correct dimensions (thereby showing the unnecessity of introducing a reaction distance into these equations as this lately has been done by many authors) and in showing the freedom we have of choosing standard states and activity scales. These choices will not affect the overall value of the rate equations, but the value of the activity term and of the exponential activation entropy term will depend in a mutually inverse way on our choice of standard states. A certain arbitrariness is hereby attached to the the standard entropy of activation. The standard heat of activation, however, is insensitive to this choice. This is a simple consequence of the standard states always being regarded ideal states or pure phases.

At equilibrium, the two mutually reverse reactions have equal rates. This is the so called exchange current i_o, which generally is a function of the reactant activities. We may therefore also define a standard exchange current J_o as the one applying to standard state activities. By multiplying (2a) with (2b) after raising these equations to a power of $1-\alpha$ and α, respectively, and using the above definitions, we easily have:

$$i_o = \frac{(\mathrm{Red})^{1-\alpha}(\mathrm{Ox})^{\alpha}}{(\mathrm{Red})_o^{1-\alpha}(\mathrm{Ox})_o^{\alpha}} J_o \qquad (3a)$$

$$J_o = nF \frac{kT}{h} c_o^{\ddagger} \exp(-\frac{\Delta G_o^{\ddagger}}{RT}) \qquad (3b)$$

where $\Delta G_o^{\ddagger}$ is defined by:

$$\Delta G_o^{\ddagger} = (1-\alpha)\,\Delta G_{o,+}^{\ddagger} + \alpha\,\Delta G_{o,-}^{\ddagger} \qquad (4)$$

and may be called the <u>mean standard (chemical) energy of activation</u> of the electrode[3,6]. As J_o also is determined by any one of the

equations (2) on putting $(Red) = (Red)_o$, $(Ox) = (Ox)_o$, and $\Delta\phi = \Delta\phi_o$, these equations are easily simplified to:

$$i_+ = J_o \frac{(Red)}{(Red)_o} \exp\left(\frac{\alpha n F(V-E_o)}{RT}\right) \qquad (5a)$$

$$i_- = J_o \frac{(Ox)}{(Ox)_o} \exp\left(\frac{(\alpha-1) n F(V-E_o)}{RT}\right) \qquad (5b)$$

when it is remembered that the difference between two electrode potentials is the same on all reference scales (i.e. $V-E_o = \Delta\phi - \Delta\phi_o$). V thus means the actual electrode potential on whatever scale one may choose, and E_o the standard potential of the electrode on the same scale.

The standard state preferred for solute reactants is that of a hypothetic (ideal) solution in which their molality (or molarity) is unity, and solid reactants are conventionally ascribed unit activity. For the standard state of the "activated complex" in electrode reactions, however, there does not seem to be any choice that so far has come into conventional use (the necessity and importance of this choice may to a large extent even seem to have been overlooked). For metal/metalion electrodes, there is one particular choice that may seem quite natural, namely:

$$c_o^{\ddagger} = n_o/N \qquad (6)$$

where n_o is the number per unit area of atomic positions in the metal surface, and N is the Avogadro number.

From (3b) and (6), we then have for the standard exchange current:

$$J_o = nF \frac{kT}{h} \frac{n_o}{N} \exp\left(\frac{\Delta S_o^{\ddagger}}{R}\right) \exp\left(-\frac{\Delta H_o^{\ddagger}}{RT}\right) \qquad (7)$$

when it is remembered that $\Delta G = \Delta H - T\Delta S$. The definition of the here used mean standard entropy ($\Delta S_o^{\ddagger}$) and heat ($\Delta H_o^{\ddagger}$) of activation is contained in (4). By not implying absolute potentials, the equations (5) and (7) give a convenient basis for the transition state treatment of the activation control of metal/metalion electrode reactions.

For any given metal, the factor n_o will depend on the crystallographic plane considered. This imposes some difficulty in the use of definition (6) when dealing with polycrystalline electrodes. In such cases, therefore, it may be more convenient to choose for the "activated complex" a standard state concentration which is independent of crystallographic orientation. This may be done by referring n_o to a given crystal plane, and, in the following application of the theory, we will refer it to the plane of closest packing. As shown above, the entropy of activation is thereby automatically also being referred to this particular choice. This does not mean, however, that the results thereby obtained necessarily apply to the close-packed plane. This would only be the case if this plane should be the only surface plane present.

The above equations may be extended in the usual way to cover also possible double layer effects on the electrode reactions[15]. As this can be proved to be inessential to the below application of the theory, this extension will not be made here.

3.0 APPLICATION OF THE THEORY

The above theory has to some extent already been used by the author in treating experimental data on the Fe/Fe^{++}_{aq} electrode[1-4], the Cu/Cu^{++}_{aq} electrode[5-8], and the Zn/Zn^{++}_{aq} electrode[9-11]. These treatments suffer somewhat, however, from a clear definition (or choice) not having been made for the standard state of the "activated complex". For this reason, and to have a closer comparison between the three mentioned metal/metalion electrodes, a brief renewed treatment will here be given.

The results referred to above show that the activation controlled reactions of these electrodes under stationary conditions all follow the Tafel law with V/lni-slopes of:

$$b_+ = -b_- = RT/2F \tag{8}$$

On the basis of (5), this gives $\alpha = 1/2$ and $n = 4$ for all these electrodes. This n-value implies that the kinetic unit equation (1) for these divalent metal electrodes should encompass <u>two</u> metal atoms and ions. On the basis of (5b), this further implies that the activation controlled rate of deposition should be proportional to the square of the metalion activity. For all these electrodes, this is satisfactorily verified and supported by direct results[1,5,9]. For iron, but not for copper and zinc, both the dissolution and the deposition reaction are moreover found to depend on pH in a way corresponding to a first order catalytic interaction of hydroxyl ions[1,4]. The kinetic unit equation (1) thus becomes:

$$2Fe + OH^- = 2Fe^{++} + OH^- + 4e^- \tag{9a}$$

$$2Cu = 2Cu^{++} + 4e^- \tag{9b}$$

$$2Zn = 2Zn^{++} + 4e^- \tag{9c}$$

for the three metal/metalion electrodes here discussed.

In the temperature range 0-40 °C, the standard exchange current is found to obey the following Arrhenius equations:

$$J_o = 8.5\ (nFT)\ 10^{12}\ \exp(-23000)RT)\ A/cm^2 \qquad (10a)$$

$$J_o = 35\ (nFT)\ \exp(-15200/RT)\ A/cm^2 \qquad (10b)$$

$$J_o = 6.1\ (nFT)\ 10^{10}\ \exp(-25400/RT)\ A/cm^2 \qquad (10c)$$

for the iron[3], copper[6], and zinc[11] electrode, respectively. Also in these equations, n is 4, and R is expressed in calorie degree^{-1} mole^{-1}. By comparing (10) with (7) and using the n_o-value[16] of $1.72 \cdot 10^{15}$ cm^{-2} for iron (the 110-plane of its b.c.c. lattice), $1.77 \cdot 10^{15}$ cm^{-2} for copper (the 111-plane of its f.c.c. lattice), and $1.63 \cdot 10^{15}$ cm^{-2} for zinc (the basal plane of its h.c.p. lattice), one obtains the following values of the mean standard heat and entropy of activation for the three electrodes:

Electrode	ΔH_o^* (kcal)	ΔS_o^* (cal/deg)
Fe/Fe^{++}	23	51
Cu/Cu^{++}	15.2	- 1.2
Zn/Zn^{++}	25.4	41.5

The mean standard heat of activation is in the above way absolutely determined, as the values ascribed to it do not refer to any arbitrary energy or potential scale, nor do they depend on the choice of standard states (see above). This makes it a most significant and important quantity in describing the behaviour of electrodes. In the case of metal/metalion electrodes, it may be even more important than this. As previously discussed[6,11], there are namely indications of it in such cases being numerically equal to the standard heat of reaction of the electrode, thereby revealing absolute values also for this latter quantity. If the suggested equality should prove to be correct, an avenue may seem open to the evaluation of absolute potentials (see Ref[11]).

The mentioned equality further implies that the separate standard heat of activation of the single electrode reactions of a metal/metalion electrode is in one direction zero (the anodic one for iron[3] and zinc[11] and the cathodic one for copper[6] in the above examples) and in the opposite direction equal to the standard heat change accompanying the kinetic unit reaction. According to (9), the latter heat change is equal to twice the standard heat of reaction.

The mean standard entropy of activation also is absolutely determined in the above way. As already described, however, it is not independent of the choice of standard states, but refers to the choices made. When conventional definitions are used for the standard states of the reactants, as mostly is the case, the activation entropy still depends on and is intimately connected to the choice made for the "activated complex". Consequently, the usefulness of the values ascribed to it directly depends on the usefulness of the latter choice. This choice, therefore, is a most important one.

The values obtained above for the mean standard entropy of activation all refer to an equivalent choice for the transition state and are therefore well suited for comparison. An interesting feature here is that the two unnoble electrodes (Fe, Zn) both show a relatively high positive mean entropy of activation, whereas this quantity for the noble electrode (Cu) is near to zero. For the latter electrode, the transition-state must in standard entropy obviously lie nearly mid-way between the two end states. For the iron and the zinc electrode, however, it can easily be shown to lie relatively near to the metallic end state. Absolute entropy data[17,18] namely show the standard entropy of reaction in cathodic direction to be 42.6 and 44.9 cal $deg^{-1} mole^{-1}$ for the iron and the zinc electrode, respectively. Thus, we here nearly have the same equality

between kinetic and thermodynamic data as discussed above for the corresponding heat terms. It would be interesting to know if the present findings for copper on the one side and for iron and zinc on the other, should be characteristic for metal/metalion electrodes with positive and negative heat of dissolution, respectively.

Double layer effects are not considered in the above treatment. This is justified by the experimental results mostly having been obtained in solutions with a large excess inert and presumably "capillary-inactive" electrolyte, and by the hydrogen evolution reaction on the metals concerned in many of the solutions applied having been found to exhibit a pH-dependence which is in accordance with what is to be expected in the absence of such effects (see Ref[15], §142). The hydrogen evolution data here referred to, have only been given for iron[1,4] and zinc[10].

4.0 CRYSTAL GROWTH CONSIDERATIONS

Metal/metalion electrodes differ from usual red/ox electrodes by the charge transfer between metal and solution being intimately connected to an equivalent mass transfer between these two phases. For solid metals, this mass transfer necessarily leads to a continuous change of the metal surface by steadily causing new surface layers to be exposed (dissolution) or formed (deposition). It seems now well recognized that this occurs by a flow of steps (boundaries of incomplete surface layers) in the surface and a flow of kinks (ends of incomplete atom rows) in the steps[19-21], the kinks being the actual lattice building and demolition sites (as first suggested by Kossel[22] and Stranski[23,24]). For liquid metals as mercury and amalgams, however, a similar change in the surface structure by the mass transfer is not to be expected for the obvious reason of their surfaces not having steps in the above sense (or - if one like - they having steps everywhere even in the absence of mass transfer). This constitutes a main difference between the two mentioned classes of metal/metalion electrodes, and may also be a main reason for differences in their kinetics.

For liquid metal/metalion electrodes, the results reviewed and discussed by Vetter[15] indicate a first-order mechanism as exemplified by the kinetic unit equation:

$$Zn\,(Hg) = Zn^{++} + 2\,e^{-} \qquad (11)$$

for the so far most extensively studied amalgam electrode. Moreover, oscillographic measurements on such electrodes have not revealed any transient behaviour attributable to possible changes in the surface structure by the mass transfer. This is in accordance with what is to be expected from general kinetic ideas and the simple picture given above of the liquid metal surface.

For solid metal/metalion electrodes, however, a second-order mechanism, as exemplified by the kinetic unit equation (9), may seem to be a relatively general one under steady-state conditions. This has now been found for manganese[25], iron[1-4], cobalt[26,27], nickel[28], copper[5-8] and zinc[9-11]. Moreover, oscillographic measurements on several of these metals (iron[29-32], cobalt[26], copper[33,34], zinc[35]) have revealed a characteristic transient behaviour (superpolarization) when going from one steady state to another (see below). On the basis of the crystal growth and dissolution theories briefly mentioned above[19-21], such a transient behaviour is not unexpected[15, 36-38], but gives indications of the reactions and the surface properties being mutually dependent, and of this dependence being responsible for the steady-state reaction order observed. The difference in behaviour of liquid and solid metal/metalion electrodes gives further indications in the same direction.

4.1 Transient and Steady States

Under galvanostatic conditions, the above mentioned superpolarization for solid metal/metalion electrodes manifests itself by the occurence of a distinct peak in the potential-time transients, somewhat as sketched in Fig. 1. The potential reaches its peak value quite rapidly, often in some milliseconds, whereafter it decays more slowly towards a steady value, which often is approximately reached first after a time of the order of seconds. In the pre-peak period, the current is composed of a capacitive ($C\ dV/dt$) and a faradaic component. At the peak ($dV/dt = 0$), the former component has died out, and the total current is faradaic (just as in the steady state). In many cases, the mass transfer occurring up to the peak does not represent more than a small fraction of a monolayer and cannot alter the surface structure very much. Under simple conditions, therefore, the corresponding

changes in faradaic current and potential from the initial steady state to the peak should represent the pure potential dependence of the reaction under approximately constant surface conditions (those applying to the initial steady state). For iron[29-31], cobalt[26], copper[33], and zinc[35], this dependence has been found to obey the Tafel law with a V/ln i-slope of numerically RT/F (as compared to RT/2F for steady-state conditions), indicating a first-order mechanism (cf. eqns. (5)) as for liquid metal electrodes. This strongly supports the above suggestion of surface changes being responsible for the steady-state reaction order observed.

In Fig. 2, the polarization behaviour just described for solid metal/metalion electrodes is schematically presented in a Tafel diagram. It is there indicated how the potential under galvanostatic conditions probably varies with the reaction rate (assumed proportional to the faradaic current) when going from one steady state to another by a single current increment (compare Fig. 1), and how this is connected to a displacement of the first-order transient Tafel line. The best support for the situation being somewhat as sketched comes from the transient data of Heusler and Cartledge[31], on iron and of Heusler[26] on cobalt. The other transient data mentioned above are not in disagreement with this sketch, but they are not comprehensive enough to show all its features. More work of this type ought therefore to be done.

In Figs. 1 and 2, the numerical overvoltage has been used (instead of merely the potential) in order to present in a simple, coinciding way the symmetric behaviour mostly found for the above mentioned metal/metalion electrodes under both steady-state and transitory conditions (when due regard is made of the starting point for the latter type of experiments[26,31]). These plots (and what is said about them) thus apply just as well to deposition as to dissolution.

The mentioned symmetry indicates the surface conditions at a steady anodic overvoltage to have the same rate effect as those at the corresponding cathodic overvoltage. That it is so and that surface changes caused by one reaction are directly applicable in affecting also the opposite reaction, may seem well verified by transient results of Heusler[26] on cobalt. These results namely show transitions between mutually corresponding steady anodic and cathodic states to occur directly and rapidly without any intermediate superpolarization. For the other metals mentioned above, transient data of this kind are still too scarce and casual to warrant a similar evaluation.

4.2 The Surface Factor

The above results clearly show the reactions of solid metal/metalion electrodes to be affected by surface changes which are slow compared to the charging of the double layer. They further show the polarization at constant surface conditions to be represented by Tafel lines for first-order reactions, and the surface changes simply to cause a displacement of these lines (see Fig. 2). This makes it possible to describe the reactions of solid metal/metalion electrodes as first-order reactions whose rate is proportional to a surface factor representing the kinetic effect of the variable surface properties.

The displacement shown by the above results for the first-order transient Tafel lines may be represented by the following partial anodic and cathodic surface factors:

$$s_+ = s_{+R} \exp\left(\frac{zF}{2RT}(V-E)\right) \qquad (12a)$$

$$s_- = s_{-R} \exp\left(\frac{zF}{2RT}(E-V)\right) \qquad (12b)$$

where z is the metal ion charge, and the subscript R refers the factors to their value at the reversible potential (V=E). From what is said above as to the effect of anodically caused surface changes on the

cathodic reaction and vice versa, one must assume both reactions to depend on one and the same total surface factor (s) being the sum of the partial ones:

$$s = s_R \cosh\left(\frac{zF}{2RT}(V-E)\right) \qquad (13)$$

This expression implies $s_{+R} = s_{-R} = s_R/2$, which has some support in the symmetry observed for the reactions, and further assumes the partial factors to be mutually independent. Support for the validity of (13) will be given below.

In Fig. 3, sketches are given of what is to be expected for the effect of metal ion activity on the position of the steady-state Tafel lines in the following two cases:

A) the surface factor at equilibrium of the electrode being proportional to the square root of the metal ion activity, and

B) it being independent of this activity.

The expectations based on A (Fig. 3A) are well borne out by experiment for all the metals mentioned above, whereas those based on B (Fig. 3B) are not. This gives:

$$s_R = a^{1/2} s_o = s_o \exp\left(\frac{zF}{2RT}(E-E_o)\right) \qquad (14)$$

where s_o is the surface factor at $a = 1$ and $V = E_o$ (E_o being the standard potential of the electrode).

On the basis of (13) and the definition of the surface factor, the absolute rate of dissolution and deposition under steady-state conditions should be given by:

$$i_+ = i_o \cosh\left(\frac{zF}{2RT}(V-E)\right) \exp\left(\frac{zF}{2RT}(V-E)\right) \qquad (15a)$$

$$i_- = i_o \cosh\left(\frac{zF}{2RT}(V-E)\right) \exp\left(\frac{zF}{2RT}(E-V)\right) \qquad (15b)$$

and the net rate of reaction by:

$$i = \pm 2i_o \cosh\left(\frac{zF}{2RT}(V-E)\right) \sinh\left(\frac{zF}{2RT}(V-E)\right) \qquad (16)$$

where plus and minus apply to positive and negative overvoltages (V-E), respectively. In Fig. 4, the functions (15) are graphically presented in a Tafel diagram. It is there also indicated how rate- and potential-corresponding points for the two mutually reverse reactions are symmetrically placed on a symmetric set of first-order transient Tafel lines (the intersection of which gives the transient exchange current applying to the common surface factor value of the corresponding points). The diagram further shows that an extrapolation of the steady-state Tafel lines to intersection (or to the reversible potential) does not directly give the value of the actual exchange current (i_o), but - according to (15) - just half this value. According to (16), however, the exchange current should be directly given by the slope of a linear i vs. zFV/RT curve at very low overvoltages. As previously pointed out by the author[5], such a difference between exchange current values determined by V/log i-extrapolations and by V/i-slopes is exactly what experimentally is found in the case of copper (the only one of the above mentioned metals for which comparable data of this kind are available). This strongly supports the validity of (13) which in the above treatment is the origin of this difference. Also the approach to potential independence shown in Fig. 4 for i_+ and i_- at cathodic and anodic overvoltages, respectively, originates from (13), and is not caused by any change in the symmetry factors.

Eqns. (12)-(14) thus represent what may be deduced for the surface factor from the mentioned transient and steady-state data. They clearly show it to be composed of an anodic and a cathodic component, both of which obey laws analogous to those for the rate of correspondingly first-order reactions at a surface with constant properties for these reactions (cf. eqns. (5) above).

4.3 The Reaction Mechanism

The results discussed above strongly indicate the reaction mechanism of the mentioned solid metal/metalion electrodes to be one for which variations in the surface structure (the step or kink density) is affecting the reactions both at low and high numerical overvoltage. If the reactions are assumed to occur via surface diffusion, this implies that the mean displacement of adatoms in the surface must be small compared to the step or kink spacing at all conditions implied. For dissolution, this compares well with what may be predicted from the edge source theory of crystal evaporation (Hirth and Pound[30]), which, for the case of steps acting as continuous line sources for diffusing adatoms, gives an approximately constant value of about 6 for the ratio between the mean step spacing and the mean displacement of adatoms. For deposition (growth), however, edges are usually not regarded a ready source for steps, which then mainly are assumed to originate from the action of emergent dislocations[20] (with a non-zero Burgers vector component normal to the surface) and from two-dimensional nucleation[19] (when sufficiently far from equilibrium). By both the dislocation and the nucleation mechanism, one should expect the above mentioned ratio to decrease with increasing cathodic overvoltage (E-V) and eventually to become smaller than 1. Thereafter, further changes in the step spacing should have only negligible effects on the growth rate. Such a transition in the deposition reaction (from dependence to independence of a surface factor) is not observed for any of the metals here considered. This fact, and even more the obvious difficulties encountered in explaining on the above basis the symmetry exhibited by these metal/metalion electrodes, make the applicability of the surface diffusion model in the present cases very doubtful. This result is in agreement with previous conclusions of Fleischmann and Thirsk[38].

Regarding then the electrochemical reactions of the metal/metalion electrodes mainly to occur directly at preferable sites (e.g. kinks in steps), one must assume the above described surface factor to represent the steady-state concentration of such sites in the surface. The laws obeyed by this factor may indicate these preferable sites to be generated by some first-order electrochemical reactions (initiation reactions) and to attain a steady-state concentration being proportional to their rate of formation and inversily proportional to the concentration of those sites at which the initiation reactions occur. If the latter sites should be surface sites of essentially invariable concentration, the mentioned inverse proportionality vanishes. This is not the case, however, if they should be sites in surface steps of variable spacing.

The initiation reactions must further constitute a small part only of the total reactions occurring. The steady-state behaviour of the electrodes should otherwise not have been of the pure second-order type observed, but rather of a mixed first- and second-order. This obviously means that the main part of the reactions must occur in a repeatable way at preferable sites generated by the intiation reactions. A chain reaction mechanism is thereby revealed for the solid metal/metalion electrodes, the reactions at preferable sites being the propagation reactions.

By this mechanism, the pH-dependence found for the iron[1-4,30,32,40] and the cobalt[26,27] electrode reactions may also seem intelligible. For iron[1,4], this dependence has been shown to obtain at pH-values at least from 0 to 14 and most probably to imply a first-order interaction of hydroxyl ions even at low pH (see eqn. (9a) above). These results may now be allowed for by assuming the hydroxyl ions to take part only in the relatively few initiation reactions occurring at sites of relatively high surface concentration.

A relatively clear picture is given above of what the propagation reactions (the main electrode reactions) are believed to be. This is not the case for the initiation reactions, however, which mainly are described as some being responsible for the surface factor and, thereby, for the concentration of kinks in the surface. As this concentration is a product of the step density in the surface and the kink density in the steps, the initation reactions may represent what is determining either one or both of these densities.

From the dislocation theory of crystal growth and dissolution[20], one should expect the steady-state density of steps to be nearly a linear function of the numerical overvoltage[36,38]. For copper, Seiter et al.[41] have found variations in the step spacing (large steps) of growth spirals and in the side slope of growth pyramides to be in accordance with this. The formation og growth spirals in electrodeposition has been observed also for a number of other metals (see e.g. Refs.[15,21,36,38]). This clearly shows dislocation sources to be operative in deposition. The formation of etch pits has often been regarded an analogous indication for dissolution. If this should be the only or the dominating step forming mechanism in the above cases, the kink density in steps must be ascribed the main role in determining the potential dependence shown by (13) and (14) for the surface factor. This further indicates the initiation reactions introduced above to be some direct electrochemical kink forming reactions at steps.

Just as for other types of chain reactions, one must also in the present case assume the steady-state concentration of chain carriers (kinks) to be determined by the balance of chain initiation and termination. A chain propagating in a step will terminate when it meets another chain or reaches a turning point or an end point of the step. The close analogy shown by (12a) and (14) for the effect of potential on the surface factor outside and at equilibrium, respectively, may indicate

the kink density in steps to have a steady-state value determined in the above way even at equilibrium of the electrode. This would imply that kinks and possibly steps are flowing in the surface also at the reversible potential, thereby allowing all step atoms and possibly all surface atoms to be exchanged with ions in the solution. For copper and zinc, radiochemical measurements have shown that all surface atoms and not only those at steps are rapidly exchanged with the solution[8].

5.0 DISCUSSION

The polarization behaviour of solid metal/metalion electrodes is clearly affected by rate influencing changes in the metal surface (step and kink density) which are responsible both for the transient superpolarization and for the steady-state second-order kinetics exhibited by electrodes of this kind. This does not only apply to the divalent metals discussed above, but possibly to most solid metal/metalion electrodes. The superpolarization has for instance been observed also for the cathodic deposition of silver on solid silver from aqueous solutions [42,43] (when the silver surface is not affected in advance by pre-polarization [43]) and for the anodic dissolution of solid silver in solid silver sulphide at higher temperatures (200-300°C) [44]. The latter shows that this characteristic behaviour is not limited to cases in which aqueous electrolytes are applied, and supports the above conclusion of it reflecting rather general and regular changes in the growth and dissolution structure of the reacting metal surface.

The rate influencing changes in the surface structure may seem to concern both the step spacing in the surface and the kink spacing in the steps. By the latter, disobedience is shown to the continuous line sink model of crystal growth and dissolution [20]. In the present work, this model has been replaced by a chain reaction model in which kinks are formed mainly by direct electrochemical initiation reactions at steps and act as chain carriers for subsequent direct electrochemical propagation reactions at kinks. In view of the uncertainty so far attached to the step spacing, no attempt has been made of carrying out a complete mathematical analysis of this model. From the above discussion of it, however, it may seem promising, and it obviously deserves further attention and elucidation.

The surface structure of a metal may also be affected by mechanical means. Deformation processes create steps in the surface and may through

the "catalytic" effect of these steps have a stronger influence on the reactions of the metal than is to be expected on purely energetic grounds. This obviously requires, however, that enough steps are created in this way to significantly increase the step density in the surface over that determined by the growth or dissolution process itself. More extra steps are thus required at high than at low overvoltages, and a given deformation process should be of decreasing importance with increasing overvoltage. As further the dissolution and growth of a crystal involve a steady generation, advance, and disappearance of steps, kinetic effects of the above type should not be expected to last very long after the step generating deformation process has ceased to operate. All these features seem well borne out by experiments (e.g. Refs. [45,46]), supporting the role ascribed to the surface structure in the reaction mechanism of metal/metalion electrodes.

In spite of the rate influencing surface changes accompanying the reactions of solid metal/metalion electrodes and of the thereby attached chain mechanism, such reactions are often not more complex than to be describable by a relatively simple kinetic reaction equation (as (9) above) with a single overall rate constant (J_o) that obeys the Arrhenius equation (as in (10) above). Of special interest here are the indications given of the Arrhenius energy being an absolute measure of the heat of reaction of the metal/metalion electrode. The author has so far not found any direct proof of this, but has shown that it for iron [6], copper [6], and zinc [11] (through an appropriate Born-Haber cycle) leads to electron evaporation enthalpies which are approximately equal to the electron work function of the respective metals. Recent results on manganese [25] indicate the same equality to apply also for this metal. This equality may thus seem a rather general and significant one for solid metal/metalion electrodes.

The Arrhenius equations (10) further show the pre-exponential factor to vary strongly for metal/metalion electrodes. For the base metals iron and zinc, it is very much higher than for the more noble metal copper. Recent results on manganese [25], however, seems to place this metal in class with copper in this respect, indicating the nobleness of the metals to have little to do with this matter. In the above treatment, the variations in the pre-exponential factor have formally been ascribed to the mean standard entropy of activation, and suggestions are given of this quantity being either near to zero (copper, manganese) or near to the numerical standard entropy of reaction of the electrode (iron, zinc). Whether this classification is a significant and sufficient one, or the variations should be due to other factors (e.g. the transmission coefficient), is difficult to say at the present stage. Even if it should be appropriate, it is not more than a classification, and it remains to explain what makes a metal belong to the one or the other of these classes.

The values used for the exchange current in the above treatment of iron, copper, and zinc have been obtained by a direct extrapolation of Tafel lines. As suggested by the crystal growth considerations and illustrated in Fig. 4, these values are probably a factor of 2 lower than the actual exchange current. By not being of much importance for the evaluation, a correction for this has not been made. Such a correction will only affect the pre-exponential factor or the activation entropy.

In the above transition-state treatment, the frequency factor kT/h of the absolute rate theory has been used. One could perhaps just as well use the molecular frequency factor of about 10^{13} sec^{-1} of the detailed rate theory, but this will not make much difference. What is of more importance in this treatment, is the choice of standard state for the "activated complex". For homogeneous reactions,

such a choice is automatically the same as for all the other reaction species, and no extra thoughts need to be given to it. For heterogeneous reactions, however, different activity scales are used for different reaction species, and extra thoughts must be paid the above choice. As the transition-state theory mainly is developed for homogeneous reactions, it is no wonder that this elementary fact to a large extent has been overlooked by many authors in applying the theory to heterogeneous reactions. The choice (6) made in the present work, may seem a reasonable one for metal/metalion electrodes and leads to interesting values for the entropy of activation (as discussed above). For ordinary red/ox electrodes, however, there are other choices that also ought to be considered (e.g. the number of moles solute per unit area in a monomolecular solvent layer of a standard 1 M solution). As pointed out above, the heat of activation is independent of the choice of standard states.

By not implying absolute electrode potentials, the equations (5) to (7) may form a recommendable basis for the transition-state treatment of activation controlled electrode reactions. The simplicity of these reactions is gained by use of the mean standard energy (heat and entropy)of activation of an electrode (defined by(4)) instead of the corresponding separate quantities for its two mutually reverse reactions. Eqns. (3) and (7) clearly show that it is this mean activation energy (heat and entropy) which is revealed by the Arrhenius equation for J_o (or i_o). For a determination of the separate anodic and cathodic components, a knowledge of absolute potentials is still required. So far, therefore, only relative values (e.g. on the standard hydrogen scale) can be given to the standard heat of activation of a single electrode reaction, whereas absolute values can be given to the mean standard heat of activation of an electrode. This is further discussed in Refs.[3,6].

In closing this discussion, it may briefly be said that our understanding of the reaction mechanism of solid metal/metalion electrodes is still far from complete. It is the hope of the author, however, that the treatment given in the present paper may assist in elucidating this matter, and that an extension of it to other metals and a pursuit of the lines of thought applied may be fruitful. This may also give results of more general importance both to the field of electrode kinetics and to the field of crystal growth. Perhaps a solution may be gained even to the old problem of absolute electrode potentials.

APPENDIX

Lower valent intermediates

Both for the Fe/Fe^{++}_{aq} and the Cu/Cu^{++}_{aq} electrode, Bockeris *et al.*[32,34] have proposed mechanisms in which monovalent species are formed as intermediates and exist in reversible equilibrium with the metal at the electrode surface whilst the redox process between divalent and monovalent species is rate controlling. This would imply that the growth and dissolution processes themselves should always occur nearly at equilibrium conditions irrespective of the actual overvoltage of the divalent metal electrode, and that this overvoltage, therefore, should be of little importance for the step spacing in the reacting metal surface. For copper, the latter is directly disproved by morphologic data of Seiter *et al.*[41], data which above are shown to be in accordance with expectations for the case of direct divalent ion transfer. This matter is otherwise discussed somewhat in Ref.[5].

ACKNOWLEDGEMENT

The author is much indebted to various members of the staff at the Central Institute for Industrial Research for valuable discussions and to the U.S. Department of Army, European Research Office, for financial support. A special gratitude goes to Director Alf Sanengen and siv.ing. B. Andvord Tönnesen for their constant encouragement and never-ending interest in this research work.

REFERENCES

1. Hurlen, T. Acta Chem.Scand. 14 (1960) 1533; Tek. Ukeblad 105 (1958) 101, 119

2. Hurlen, T. Acta Chem.Scand. 14 (1960) 1555

3. Hurlen, T. Acta Chem.Scand. 14 (1960) 1564

4. Hurlen, T. and Haraldsen, B. to be published

5. Hurlen, T. Acta Chem.Scand. 15 (1961) 630

6. Hurlen, T. Acta Chem.Scand. 15 (1961) 621

7. Hurlen, T. Acta Chem.Scand. 15 (1961) 615

8. Hurlen, T. and Lunde, G. to be published

9. Hurlen, T. Acta Chem.Scand. 16 (1962) 000; Electrochemical Behaviour of Zinc, Central Institute for Industrial Research, Oslo, January 1962, Chapter I.

10. Hurlen, T. Acta Chem.Scand. 16 (1962) 000; Electrochemical Behaviour of Zinc, Central Institute for Industrial Research, Oslo, January 1962, Chapter II.

11. Hurlen, T. Acta Chem.Scand. 16 (1962) 000; Electrochemical Behaviour of Zinc, Central Institute for Industrial Research, Oslo, January 1962, Chapter III.

12. Hurlen, T. Acta Chem.Scand. 15 (1961) 1231; ibid 15 (1961) 1239; ibid 15 (1961) 1246; ibid 16 (1962) 279.

13. Parsons, R. Trans.Faraday Soc. 47 (1951) 1332.

14. Bockris, J.O'M. Modern Aspects of Electrochemistry, Butterworths, London 1954, Chapter IV.

15. Vetter, K.J. Electrochemische Kinetik, Springer, Berlin/Göttingen/Heidelberg 1961.

16. Pearson, W.B. Handbook of Lattice Spacings and Structures of Metals, Pergamon Press, London/New York/Paris/Los Angeles 1958.

17. Latimer, W.M. Oxidation Potentials (2nd. ed.), Prentice-Hall, New York 1952

18. deBethune, A.J., Licht, T.S., and Swendeman, N. J.Electrochem.Soc. 106 (1959) 616

19. Volmer, M. Kinetik der Phasenbildung, Verlag Steinkopff, Dresden/Leipzig 1939

20. Burton, W.K., Cabrera, N., and Frank, F.C. Phil.Trans.Royal Soc. London A 243 (1951) 299

21. Doremus, R.H., Roberts, B.W., and Turnbull, D. Growth and Perfection of Crystals (Proc. of an International Conference on Crystal Growth held at Cooperstown, New York, 1958), Wiley, New York 1958.

22. Kossel, W. Nachr.Ges.Wiss.Göttingen, math.-physik. Kl.(1927) 135

23. Stranski, I.N. Z.physik.Chem. 136 (1928) 259

24. Knacke, O. and Stranski, I.N. Erg.exact.Naturw. 26 (1952) 383

25. Hurlen, T. and Våland, T. to be published

26. Heusler, K.E. Z.Electrochem. 66 (1962) 177

27. Hurlen, T. and Leinum, M. to be published

28. Hurlen, T. to be published

29. Rojter, W.A., Juza, W.A., and Polujan, E.S. Acta Physicochim. USSR 10 (1939) 389

30. Heusler, K.E. Z.Electrochem.62 (1958) 582

31. Heusler, K.E. and Cartledge, G.H. J.Electrochem.Soc. 108 (1961) 732

32. Bockris, J.O'M, Drazic, D., and Despic, A.R. Electrochim.Acta 4 (1961) 325

33. Kravtsov, V.J. Zhur.Fiz.Khim. 33 (1959) 165

34. Mattsson, E. and Bockris, J.O'M. Trans.Faraday Soc. 55 (1959). 1586

35. Rojter, W.A., Polujan, E.S., and Juza, W.A. Acta Physicochim. USSR 10 (1939) 845

36. Vermilyea, D.A. J.Chem.Phys. 25 (1956) 1254

37. Lorenz, W. Z.physik.Chem. Neue Folge 17 (1958) 136; Z. Naturf. 9A (1954) 716; Z.Elektrochem. 57 (1953) 382

38. Fleischmann, M. and Thirsk, H.R. Electrochim.Acta 2 (1960) 22

39. Hirth, J.P. and Pound, G.M. J.Chem.Phys. 26 (1957) 1216; J.Phys.Chem. 64 (1960) 619

40. Christiansen, K.A., Høeg, H., Michelsen, K., Nielsen, G.B., and Nord, H. Acta Chem.Scand. 15 (1961) 300.

41. Seiter, H.,Fischer,H. and Albert, L. Electrochim.Acta 2 (1960) 97

42. Mehl, W. and Bockris, J.O'M. Canad.J.Chem. 37 (1959) 190

43. Schottky, W.F. Z.physik.Chem. Neue Folge 31 (1962) 40

44. Rickert, H. and O'Briain, C.D. Z.physik.Chem. Neue Folge 31(1962)71

45. Gerischer, H. and Rickert, H. Z.Metallkunde 46 (1955) 681

46. Windfeldt, A. and Hurlen, T. Effect of Plastic Flow on the Electrochemical Behaviour of Copper, Annual Report B-1179, Royal Norwegian Council for Scientific and Industrial Research, February 1962; Windfeldt, A. Tidsskr.Kjemi, Bergv., Metallurgi 21(1961)22.

FIGURES

Fig. 1. Typical galvanostatic transients for solid metal/metalion electrodes.

Fig. 2. Transient and steady-state Tafel lines for solid metal/metalion electrodes.

Fig. 3. Effect of the metal ion activity on the position of the Tafel lines for solid metal/metalion electrodes in the cases of (A) s_R being proportional to the square root of this activity and (B) s_R being independent of it.

Fig. 4. Tafel diagram presentation of the rate equations (15). The axis are divided in ln-units and in units of 2RT/zF, respectively.

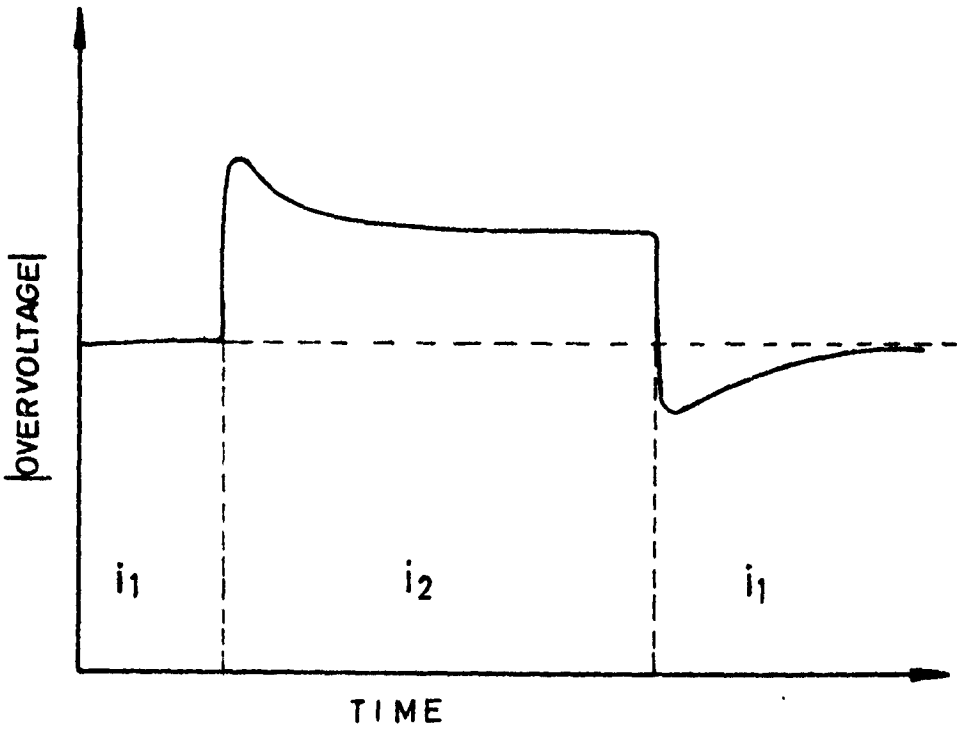

Fig. 1

Typical galvanostatic transients for solid metal / metalion electrodes.

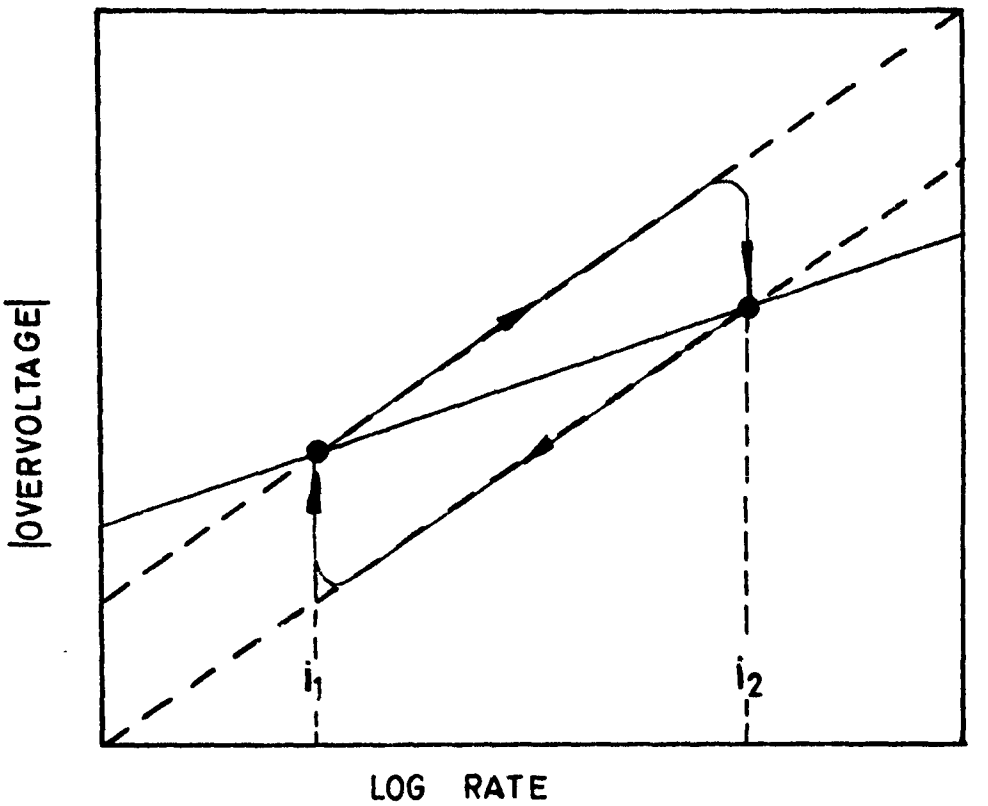

Fig.2 Transient and steady-state Tafel lines for solid metal/metalion electrodes.

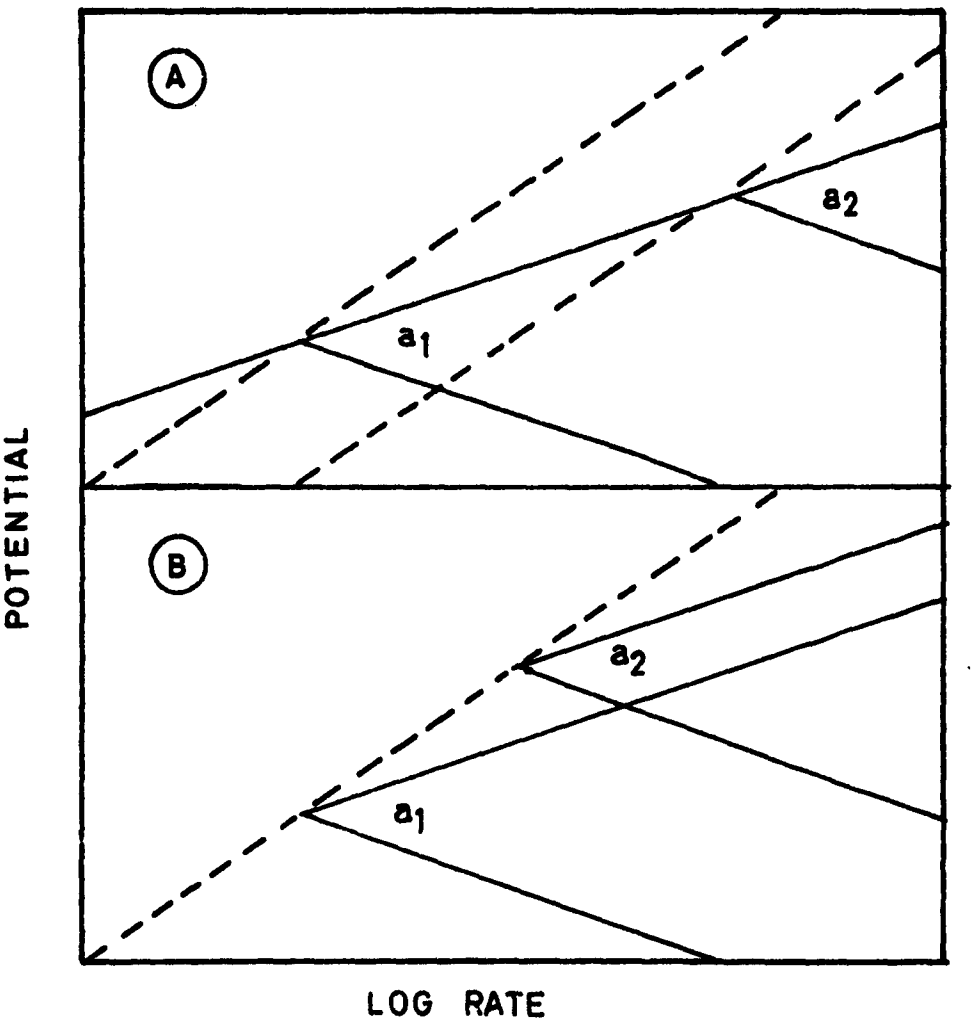

Fig.3

Effect of metal ion activity in case of A) s_R being proportional to its square root and B) s_R being independent of it.

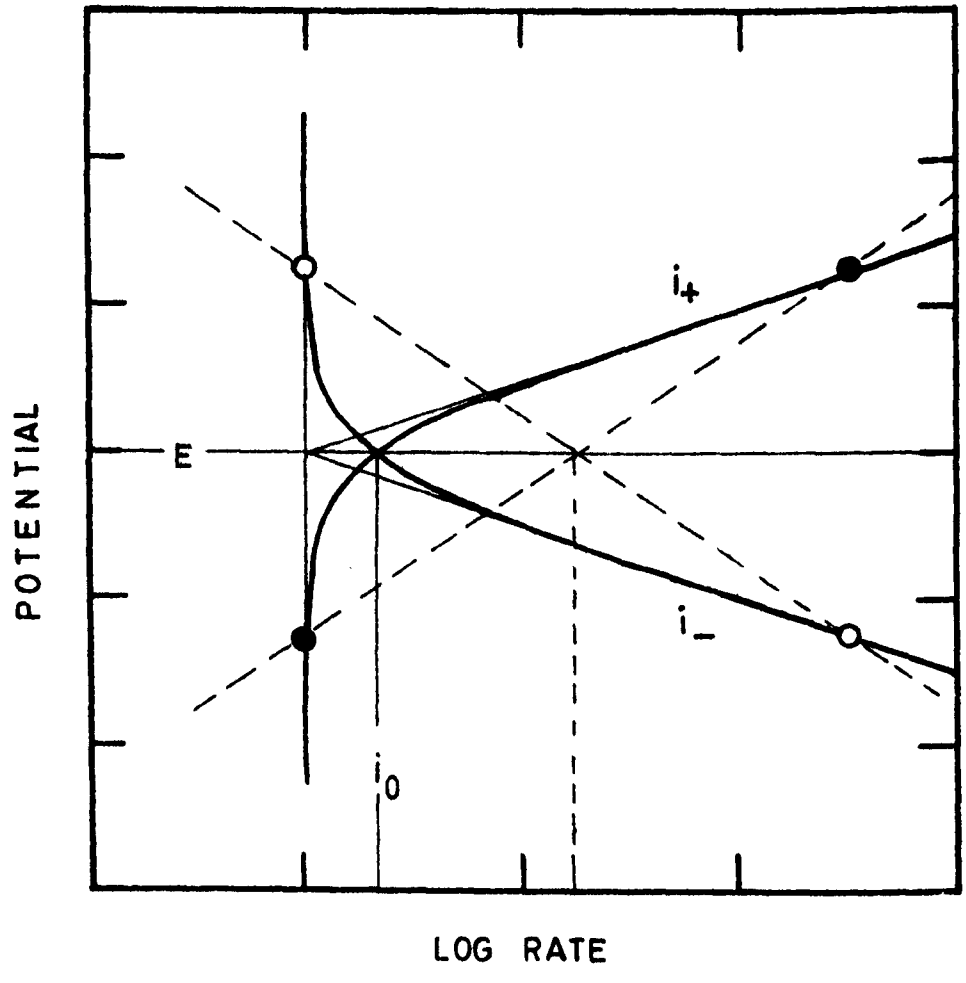

Fig.4

Tafel diagram presentation of the rate equations (15). The axis are divided in ln-units and in units of 2RT/zF, respectively.